Investigation of the role of cytoskeleton protein KATNAL2 in ribosomal gene transcription in mouse cells

KYRIAKI M. TIMOTHEOU

A Research-Based Master's Thesis
for the
Degree of Magister Scientiae in Biomedical Sciences

May 23, 2023

ABSTRACT

The discovery that katanin-like cytoskeleton protein KATNAL2, in addition to its intracellular localization at MTs and sites associated with MTs (centrioles, cilia), also, unexpectedly, resides in the nucleolus, suggests an additional putative function to its role in the cytoskeleton. KATNAL2 is highly enriched in the nucleolus, particularly in the chromatin fraction, similar to nucleolar proteins UBF, fibrillarin, treacle and RNA Pol.I, suggesting that KATNAL2 is bound to chromosomal rDNA. Here we investigate the quantification of rRNA expression and explore the role of KATNAL2 in ribosomal gene transcription. As a complement to other approaches, such as Northern blot and quantitative RT-PCR, standard methods used by members of the host laboratory to measure rRNA expression levels, here brief labeling of cells with 5-fluorouridine (FUrd) incorporated into nascent RNA, as a nucleoside analog, was used to quantify total rRNA synthesis. Wild-type NHI 3T3 mouse fibroblast cell line and 2 derivative silenced-KATNAL2 clones, clone 2.43 and clone 8-8, were cultured in three different serum concentrations of 0.5% (restrictive growth media), 10% (normal growth media), and 20% (enriched growth media) and exposed to FUrd. A dataset of 1200 cells in total was analysed (600 cells in total for WT, 300 cells in total for clone 2.43 shKATNAL2 cells and 300 cells in total for clone 8-8shKATNAL2 cells, i.e. 100 cells per growth condition per cell line).The quantitative assessment and statistical evaluation included analysis of FUrd intensity as a proxy for rRNA transcription, nucleolar and nuclear size, number of nucleoli per cell, and FUrd intensity/size of the nucleolus. The IMARIS software was utilized for extracting measurements from microscope images (previously acquired by PhD student Andria Theophanous). Quantification and statistical evaluation were performed with GraphPad Prism. The findings revealed increased rRNA levels in silenced KATNAL2 cells, compared to WT cells, in step with serum concentration increases and at all serum concentrations. Additionally, there was a remarkable increase in the size and number of nucleoli in the absence of KATNAL2 protein, in relation to wild-type cells. Changes in nuclear size were also observed in silenced KATNAL2 cells compared to wild-type cells. Overall, these results are consistent with a role of KATNAL2 in rRNA transcription.

Keywords: rRNA transcription, FUrd, nucleolus, nucleus, FUrd intensity, KATNAL2

ACKNOWLEDGEMENTS

I want to thank my thesis supervisor Dr Niovi Santama for the essential guidance she provided me throughout the completion of my thesis. Also, I want to thank the PhD candidate Andria Theophanous who supported me from the beginning of my thesis until the end and gave me important information to complete my thesis.

Moreover, I would like to thank the Committee Members of this thesis, Dr Chrysoula Pitsouli and Dr Pantelis Georgiades, who agreed to participate in my thesis presentation and grade the total effort.

Finally, many thanks to my family, friends and my fiancé for their continued support and love.

COMPOSITION OF THE EXAMINATION COMMITTEE

Thesis Supervisor (Examination Committee coordinator):Niovi Santama, Dept. of Biol. Sciences, UCY

Committee Member:Chrysoula Pitsouli, Dept. of Biological Sciences, UCY

Committee Member:Pantelis Georgiades, Dept. of Biological Sciences, UCY

University of Cyprus
Department of Biological Sciences

Master Research Dissertation in Biomedical Sciences (BIO 830/600)

Student Presentation

Tuesday, 23 May 2023 at 08:00
Building CTF 01, Room 004, Panepistimioupoli Campus

This seminar is open to the public

Kyriaki M Timotheou

Thesis Supervisor: Prof. Niovi Santama

"Investigation of the role of cytoskeleton protein KATNAL2 in ribosomal gene transcription in mouse cells"

The discovery that katanin-like cytoskeleton protein KATNAL2, in addition to its intracellular localization at MTs and sites associated with MTs (centrioles, cilia), also, unexpectedly, resides in the nucleolus, suggests an additional putative function to its role in the cytoskeleton. KATNAL2 is highly enriched in the nucleolus, particularly in the chromatin fraction, similar to nucleolar proteins UBF, fibrillarin, treacle and RNA Pol.I, suggesting that KATNAL2 is

bound to chromosomal rDNA. Here we investigate the quantification of rRNA expression and explore the role of KATNAL2 in ribosomal gene transcription. As a complement to other approaches, such as Northern blot and quantitative RT-PCR, standard methods used by members of the host laboratory to measure rRNA expression levels, here brief labeling of cells with 5-fluorouridine (FUrd) incorporated into nascent RNA, as a nucleoside analog, was used to quantify total rRNA synthesis. Wild-type NHI 3T3 mouse fibroblast cell line and 2 derivative silenced-KATNAL2 clones, clone 2.43 and clone 8-8, were cultured in three different serum concentrations of 0.5% (restrictive growth media), 10% (normal growth media), and 20% (enriched growth media) and exposed to FUrd. A dataset of 1200 cells in total was analysed (600 cells in total for WT, 300 cells in total for clone 2.43 shKATNAL2 cells and 300 cells in total for clone 8-8shKATNAL2 cells, i.e. 100 cells per growth condition per cell line).The quantitative assessment and statistical evaluation included analysis of FUrd intensity as a proxy for rRNA transcription, nucleolar and nuclear size, number of nucleoli per cell, and FUrd intensity/size of the nucleolus. The IMARIS software was utilized for extracting measurements from microscope images (previously acquired by PhD student Andria Theophanous). Quantification and statistical evaluation were performed with GraphPad Prism. The findings revealed increased rRNA levels in silenced KATNAL2 cells, compared to WT cells, in step with serum concentration increases and at all serum concentrations. Additionally, there was a remarkable increase in the size and number of nucleoli in the absence of KATNAL2 protein, in relation to wild-type cells. Changes in nuclear size were also observed in silenced KATNAL2 cells compared to wild-type cells. Overall, these results are consistent with a role of KATNAL2 in rRNA transcription.

TABLE OF CONTENTS

INTRODUCTION

1.1 Investigation of KATNAL2 (Katanin-like-2) in mouse cells

The host laboratory identified a new family of Katanin-like 2 (KATNAL2) proteins in mouse, consisting of five alternative isoforms encoded by the KATNAL-2 genomic locus (Ververis et al., 2016). In experiments, in order to identify proteins that interact with the Nubp1 protein, five separate cDNAs containing the open reading frame (ORF) for alternatively spliced products of the KATNAL2 genomic locus were identified, ranging in size from 1.62 to 1 ,12 kbp. The KATNAL2 gene is located on chromosome 18 of the mouse and consists of 16 exons, thanks to which the alternative splicing of the isoforms takes place. The five isoforms of the KATNAL2 protein family are referred to as: Katnal2-L1, Katnal2-L2, Katnal2-L3, Katnal2-S1, and Katnal2-S2. All five alternative KATNAL2 isoforms manage to encode katanin p60-like proteins bearing the typical sequence elements of the Katanin protein (AAA, MT-binding, and Walker motif). These isoforms range in expected molecular weights between 41.8 and 61.1 kDa, with sequence variations near their N-terminus, and with three of them bearing a characteristic LisH motif, MT-binding, or protein-protein interactions with the ATPases.
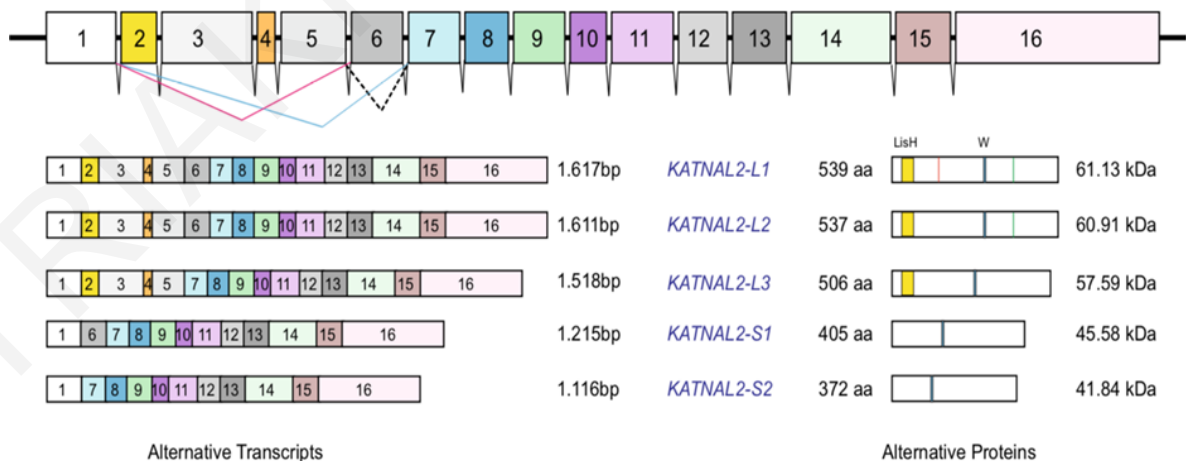

Alternative Transcripts   Alternative Proteins

Figure 1.1: Depiction of the KATNAL2 gene on mouse chromosome 18 and the appearance of its five isoforms through alternative splicing

The 16 exons of KATNAL2 are represented with different colours each. The five different cDNAs correspond to isoforms designated as Katnal2-L1, L2, L3, S1 and S2, resulting from alternative splicing of the 16 exons. The L1 and L2 isoforms differ only by two additional amino acids (V, K) in L1, and their position is marked with a red line in L1. The various motifs are highlighted in colours such as yellow for the LisH region, the Walker motif as blue and SNPs in L1 and L2 in green. (Figure from Ververis et al., 2016).

KATNAL2 is localized to interphase microtubules, centrosomes, the mitotic spindle, interbody, and cilia. Through immunofluorescence experiments in mouse NIH 3T3 and IMCD cells using dual labeling combinations, i.e., anti-KATNAL2 together with anti-γ-tubulin antibody, revealed localization of KATNAL2 associated with the cytoskeleton. It was observed that during interphase, the concentration of KATNAL2 immunoreactivity in centrosomes was specifically moderate, the protein was enriched in centrioles in the center of MT stars at the onset of mitosis (prophase and prometaphase) and in later mitotic phases. KATNAL2 was also detected specifically in cilia, both in the axon and in the basal body. KATNAL2 affects the number of centrioles, is involved in cytokinesis and at the same time in the progression of the cell cycle. MTs and centrosomes in interphase cells, the mitotic spindle and centrosomes at its poles were found to be prominent localization sites of KATNAL2 proteins. Next, the researchers sought to understand the functional role of KATNAL2 at these sites in various cell lines by regulating its concentration in vivo. Efficient downregulation of Katnal2 was achieved by selection and screening of isolated, permanently silenced clones, that showed silencing phenotypes. The silenced cells had a significantly larger overall size. In conclusion Katnal2 downregulation appears to affect MT-based structures throughout the cell cycle and likely has an impact on the cell cycle itself. These findings are consistent with different aspects of MT-based Katanin function in distinct biological processes (Ververis *et al*., 2016).

Another finding in the study of the KATNAL2 protein was its involvement in ciliogenesis. NIH 3T3 cells were silenced and tested for the formation of sensory cilia by depriving them of a condition and compared with those growing in parallel in enriched growth media. It was observed that induced silenced cells had essentially the same, low ratio of basal levels of ciliated cells as control cultures growing in complete media. These results suggest that, with KATNAL2 deficiency, there is a reduction in the propensity for ciliogenesis or in the stability of newly formed cilia, resulting in a reduced population of ciliated cells. This was

followed by evaluation of the effect of increased expression of KATNAL2 on ciliogenesis by overexpression of KATNAL2 by transient transfection. Overexpression of the tagged forms of either KATNAL2-L1 or KATNAL2-S1 or their combination results in severe cell apoptosis, mislocalization and aggregation of KATNAL2 into large cytoplasmic inclusions. These observations, combined with observations of siRNA-mediated silencing, led to the hypothesis that, in vivo, KATNAL2 protein levels are tightly regulated and that altering its expression levels to very low or high levels can become toxic to the cells (Ververis *et al*., 2016).

An alternative strategy that was tested was the construction of IMCD cell lines that permanently express either Cherry-KATNAL2-S1 or -L1 fusion proteins after integration into the genome. The two KATNAL2-expressing populations S1 and L1 showed a reduced mitotic index. Nevertheless, all stable clones maintained a good proliferation rate, normal morphology, stable but moderate expression and correct localization of KATNAL2 proteins. By combining all these together, the final balance of KATNAL2 activity may be critical for the control of many processes involving microtubules, including centroid number, cell division, cytokinesis, and cell and nuclear size (Ververis *et al*., 2016).

1.2 Study of KATNAL2 in *Xenopus* embryos

The research of KATNAL2 in mice, provided a greater impetus for further study and for this, members of the host laboratory turned to the exploration of vertebrate development with particular interest in the nervous system where Katanin proteins are related to human diseases. For example, mutations in the p80 subunit of Katanin (KATNB1) cause severe disturbances in cortical development and microcephaly, and KATNAL2 has been identified as a risk gene for autism spectrum disorders (ASD) in patient sequencing studies (Willsey *et al.,* 2018).

In the host laboratory study, *Xenopus* embryos were used to functionally characterize the developmental roles of KATNAL-2 in vivo, participating in neurological development (Willsey *et al.,* 2018. Evidence shows that KATNAL-2 was expressed in a wide range of tissues including neural tissues throughout development, was localized to cilia axons, basal bodies, centrioles, and axons, and was required for ciliogenesis and proper brain development (Willsey et al., 2018). Two KATNAL2 isoforms of *X. tropicalis* were identified which displayed the typical elements of the Katanin protein sequence (AAA, MT-binding and Walker motif), with the smaller isoform lacking a 32 amino acid sequence encoded by exon 6. Both isoforms had

the LisH motif, which as previously mentioned, are an important sequence for protein-to-self interactions. During *X. tropicalis* embryo development it was revealed that both KATNAL2 isoforms are maternally inherited as well as being expressed by the embryo after the initiation of zygotic transcription at developmental stage 9. During gastrulation, KATNAL2 was present in the dorsal lip of blastopore, including dorsal mesoderm; Furthermore, during neurulation, strong KATNAL-2 expression was observed in the notochord and relatively low expression was detected in the neural floor plate. Expression was also observed in the epidermis (stage 30 and later) and was more prominent in the notochord and brain, and additional staining was observed in the developing nephrosomes, otic vesicles and pharyngeal arches, the developing brain as well as the expression of KATNAL2 was strong in cells lining the ventricles (Figure 1.2) (Willsey *et al.,* 2018).

Figure 1.2: Expression of KATNAL2 in tissues and nervous system at various developmental stages.
A) KATNAL2 expression is enriched in the dorsal mesoderm (dm). A′) Transverse section of A. B) Dorsal view of
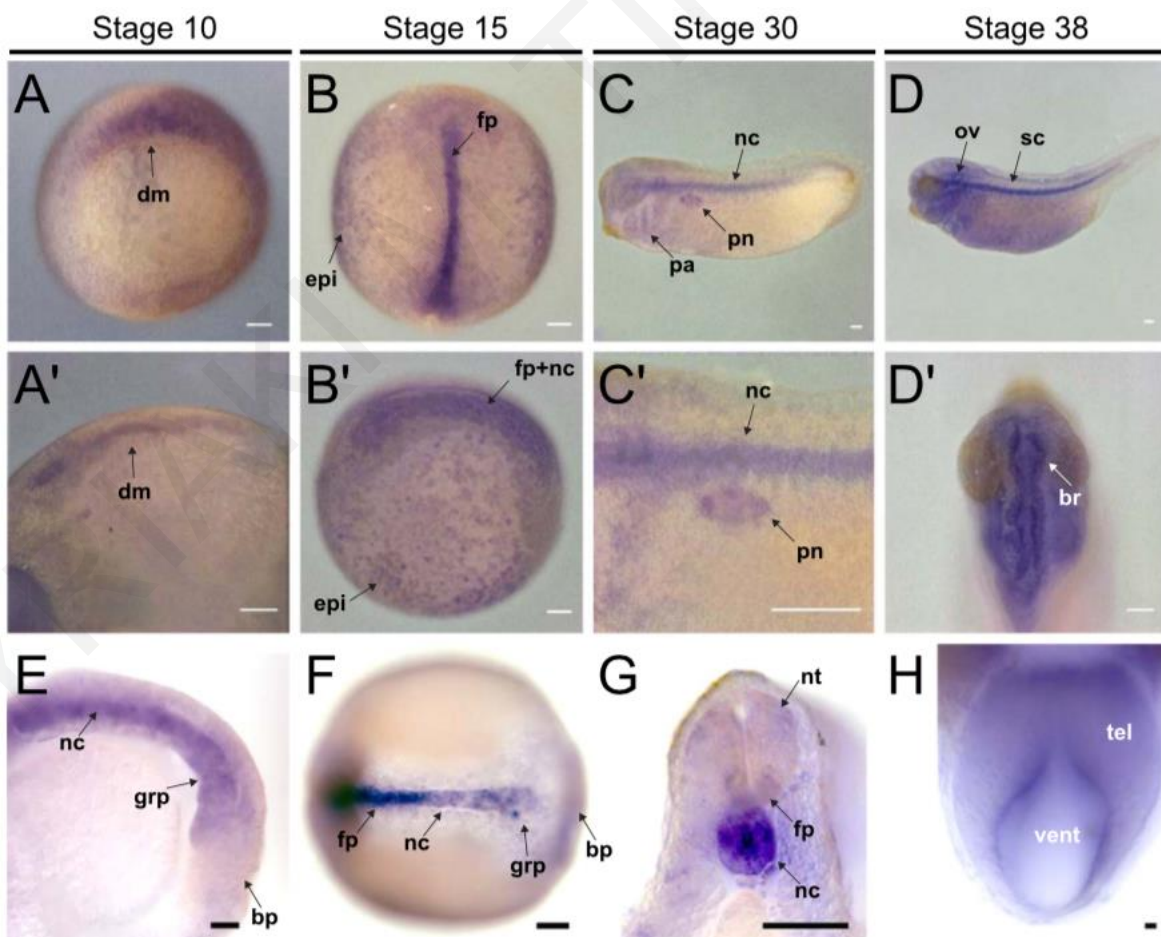
KATNAL2 expression in floor plate (fp) and epidermis (epi). B) Lateral view of B, showing the notochord (nc). C)

Lateral view of KATNAL2 expression enriched in nc, prerenal nephrosomes (pn) and pharyngeal arches (pa). C') Higher magnification view of C highlighting pn and nc expression. D) Lateral view of katnal2 expression in spinal cord (sc) and otic vesicle (ov). D) Dorsal view of katnal2 expression in the brain (br), specifically in cells lining the ventricles. E) Sagittal section of stage 15 embryo showing gastroceol roof plate (grp) expression anterior to the blastopore (bp). F) Coronal section showing an inner dorsal view of a stage 15 embryo, with expression in nc and grp. G) Transverse section of a stage 30 embryo showing expression in the neural tube (nt), floor plate (fp) and notochord (nc). H) Stage 38 embryo showing high expression in cells lining the telencephalic (tel) and ventricle (ven) (Figure from Willsey et al., 2018).

To localize KATNAL2 in vivo, antibodies against the protein were used. In epidermal cells of *X. tropicalis,* localization of KATNAL2 was observed in the axons of cell cilia, in the basal bodies of multiciliated cells, in the centrioles of non-ciliated cells as well as in the midbody in dividing cells. In the XL177 cell line, protein expression was localized to centrioles, mitotic spindles, basal bodies, and cilia. Later on, at the 45-cell stage the protein was widely expressed but enriched in cells with a high concentration of cilia such as those lining the first ventricle of the brain. KATNAL2 is required in ciliogenesis and brain development as defective ciliogenesis was observed after application of the CRISPR method or reduction of gene expression by using specialized morpholinos. More specifically, targeted multiciliated cells showed reduced ciliogenesis and remaining cilia appeared smaller in size than non-targeted multiciliated cells in both X. tropicalis and X. laevis species. Loss of KATNAL2 protein function causes reduced size in the brain and specifically in the telencephalon region (Willsey *et al.,* 2018).

The general observations that emerged through the study of KATNAL2 in frog embryos are that KATNAL2 expression is highly enriched in developing skin, kidney, brain, eye, and inner ear, all tissues where it is known to be strongly ciliogenesis. Katnal2 protein is localized to basal bodies, axons of cell cilia, centrioles, and mitotic spindles, and in many developing tissues. And consequently, loss of KATNAL2 function causes a deficiency in ciliogenesis (Willsey *et al.,* 2018)

1.3 Localization of KATNAL-2 into the nucleolus

After extended work and research, members of the Santama laboratory discovered that, in addition to KATNAL2 being detected intracellularly at MTs and locations associated with MTs (centrioles, cilia), a portion of KATNAL2 (unexpectedly) resides in the nucleolus. This implies that it serves a purpose other than in the cytoskeleton. KATNAL2 was localized in the nucleoli of mouse NIH 3T3 cells (and other cells) in a punctate pattern, close to or overlapping with the rRNA transcriptional activator UBF and the rRNA methyltransferase fibrillarin (proteins that are markers of the nucleolus' fibrillar component (FC) and dense fibrillar center (DFC)). KATNAL2 was found in the same immunofluorescent foci on chromosomes as UBF during mitosis, when UBF (but not fibrillarin) is kept attached to chromosomes at rDNA loci. They validated KATNAL2 nucleolar localization utilizing antibody-independent methods, such as transient transfection by electroporation in cultured cells and in vivo via mRNA microinjection in *Xenopus* embryos (unpublished results).
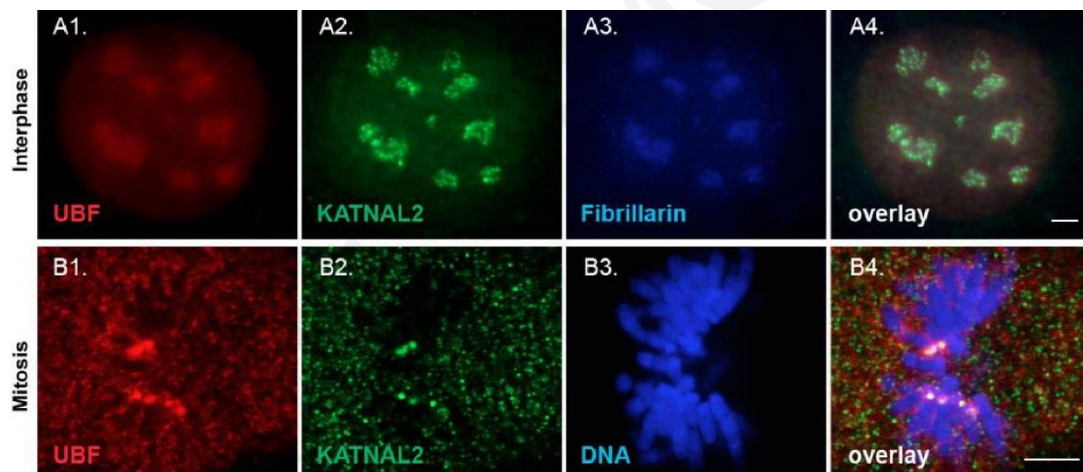

Figure 1.3: In an interphase cell, KATNAL2 co-localizes in the nucleolus with UBF and fibrillarin; moreover, immunofluorescence shows that KATNAL2 co-localizes with UBF on condensed mitotic chromosomes.

(A series) Co-localization of KATNAL2 (green; A2) with UBF (red; A1) or fibrillarin (blue; A3) at interphase. Overlay in A4.

(B series) Co-localization of KANAL2 (green; B2) and UBF (red; B1) in foci dispersed over several condensed mitotic chromosomes (blue; B3). Overlay in B4.

Scale bars 10 μm (A series), 5 μm (B series) (Figure from unpublished results of Santama's laboratory).

In accordance with these results, biochemical fractionation of NIH 3T3 fibroblast extracts, assessing total cell extract, nuclear, nucleoplasmic, nucleolar, and chromatin fractions by Western blot, revealed that, in addition to cytoplasmic KATNAL2, a further portion of KATNAL2 is highly enriched in the nucleolus and, particularly, in the chromatin fraction, similarly to nucleolar proteins UBF and Fibrillarin. Parallel precipitation of HeLa nuclear extracts with ammonium sulfate, showed co-fractionation of KATNAL2 with its associated protein Nubp1, as well as nucleolar proteins involved in rRNA transcription and processing (UBF, fibrillarin, treacle, RNA PolI), histones, and Lamins A/C. Alongside, a confocal study of nucleoli in KATNAL2-silenced cells revealed that silencing of KATNAL2 resulted in severe morphological alterations in the structure of the nucleoli. Nucleoli were increased in contrast to wild-type, DFC marker protein fibrillarin was more peripherally localized, and heterochromatin masses surrounding the nucleoli were significantly decreased. Subsequent electron microscopy studies have corroborated alterations in the fine structure of nucleoli and indicated that the DFC had risen at the expense of the FC (unpublished results).

Employing ChIP assays for KATNAL2, UBF, and RNA Pol.I, it was demonstrated that KATNAL2 binds many locations within the rDNA cassette in a manner that overlaps with UBF and RNA Pol.I binding. Subsequently, by comparing the binding patterns of wild-type cells and cells from a KATNAL2 silenced clone, it was discovered that the downregulation of KATNAL2 and consequent reduction of its binding within the rDNA chromatin was accompanied by a corresponding marked reduction of UBF binding across the rDNA cassette and a concurrent reduction of rRNA transcription, as evidenced by reduced RNA Pol.I binding at promoter's sequences (unpublished results).

There are currently being conducted metabolic labelling investigations in order to compare wild type and KATNAL2-silenced cells with the aim to quantify the pre rRNA and main processing rRNA species. Initial Northern blot analysis showed probable rRNA processing defects in the absence of KATNAL2, and they are presently doing a detailed quantitative investigation of the 47S rRNA and major rRNA species to assess rRNA processing (unpublished results).

1.4 The nucleolus

In eucaryotes, the nucleolus is the most prominent membraneless compartment in the nucleus and is renowned as the location of ribosome biogenesis. The existence of the nucleolus has been described for more than two centuries; the name nucleolus originated in 1839 and means "small nucleus." However, it took more than a century to comprehend the structure and function of the nucleolus (Lo *et al.,* 2006, Pederson., 1998). The main function of the nucleolus is the synthesis and processing of rRNA and ribosome assembly. Moreover, the nucleolus serves as a key center for various nuclear and cellular functions. For example, the movement of chromatin towards or away from the nucleolus can activate and silence gene transcription, mediate chromatin domain inactivation, underpin allelic exclusion, and spatially organize gene recombination. Protein movement between the nucleolus and the nucleoplasm, in turn, governs DNA repair, RNA Pol II transcription, telomere maintenance, the stress response, and apoptosis. Dynamic changes in the location of various proteins and chromatin mediated by the nucleolus appear to affect a wide range of previously unrelated activities. Also, the nucleolus has been demonstrated to be involved in additional roles, some of these include, tRNA modifications, and viral life-cycle management. Furthermore, defects in many of these processes, have been connected to human diseases including neurodegeneration and cancer, as well as natural processes like aging (Iarovaia *et al.,* 2019, Hernandez-Verdun *et al*., 2010).

1.4.1 The structure of nucleolus

Additionally, the nucleolus is surrounded by the peri-nucleolar heterochromatin (PH) (Villacís *et al.,* 2018*).* The nucleolus forms around the clusters of 200-400 genes coding for ribosomal RNAs arranged in a tandem array, and the transcriptional activity of ribosomal genes in the nucleolus gives rise to its characteristic ultrastructural organization: the fibrillar center (FC), surrounded by the dense fibrillar component (DFC), which is bordered by the granular component (GC). In non-transformed human cells, these genes localize to the short arms of five acrocentric chromosomes (13,14,15,21,22), forming the nucleolar organizer regions (NORs) (Salvetti and Greco., 2014)

The architecture of the nucleolus among yeast, amphibians and mammals differs (Hori *et al*.,2023). FCs are clear fibrillar zones with fibrils that range in size from 0.1 to 1 m. They

15

are surrounded in part by a highly contrasting DFC with a compact texture. The FCs and DFC are embedded in the GC, which mostly comprises of granules 15-20 nm in diameter in a loosely organized distribution. A spatiotemporal map of ribosome biogenesis in these three nucleolar components was obtained using complementary approaches, including the localization of rDNAs, rRNAs, small nucleolar RNAs (snoRNAs), as well as several proteins belonging to transcription and processing machineries and ribosomal proteins. It was discovered that active pol I transcription sites are located at the interface between the FCs and the DFC, where early pre-rRNA processing occurs in the DFC and late processing occurs in the GC (Hernandez *et al.*, 2010).
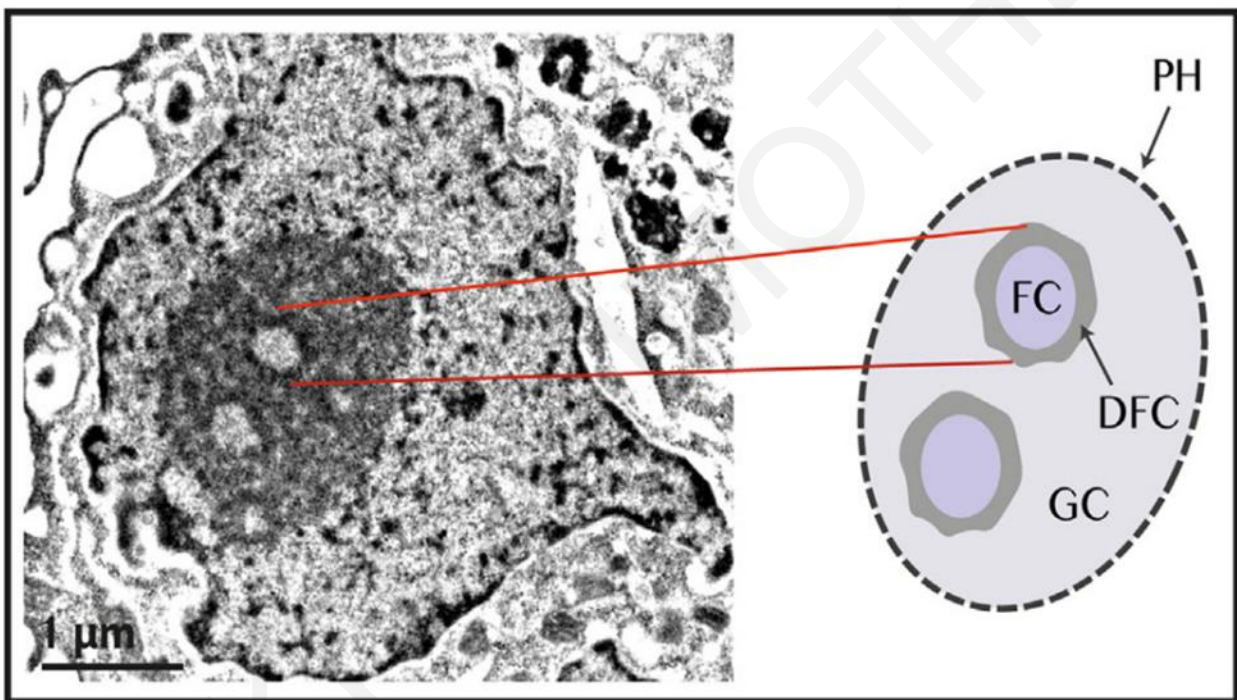
Figure 1.4.1 Structure and components of nucleolus

An MV4-11 cell imaged using transmission electron microscopy. Although some of the RNA Polymerase (Pol I) transcription components required for transcription are present, the fibrillar center (FC) contains inactive or silent rRNA genes (rDNA). The dense fibrillar component (DFC), which surrounds the FC and is rich in pre-rRNA synthesis and early processing components, surrounds the FC. The late processing factors and rproteins are found in the granular component (GC), which surrounds the FC/DFC. The nucleolus is surrounded by peri-nucleolar heterochromatin (PH) (Villacís et al.,2018).

1.4.2 How the nucleolus assembles and disassembles during the cell cycle

In cycling cells, nucleoli assembled at the exit from mitosis, they are functionally active throughout interphase, and they disassemble at the beginning of mitosis (Hernandez-Verdun *et al.*, 2010). In mammals, the structure of the nucleolus varies with the stages of the cell cycle. In prophase a disorganization of the nucleolus is observed, and it reassembles at the end of the mitotic process. Maximum transcriptional activity in the nucleolus has been observed in the S and G2 phases (Leung and Lamond., 2003).

In the early G1 phase of the cell cycle, nucleoli form as several smaller units that subsequently consolidate into 1-2 larger functional nucleoli containing multiple NORs. The nucleoli are now connected with PH generated from DNA adjacent to the NORs. The rate of ribosomal gene (rDNA) transcription does not peak until S phase and continues to be enhanced in G2 until the nucleoli disintegrates at the conclusion of mitosis. Interestingly, a number of nucleolar proteins, such as upstream binding transcription factor (UBTF, also known as UBF), remain connected with the rDNA during mitosis. Disassembly in M phase is induced in part by cyclin dependent kinases (CDK), especially CDK1-cyclin B phosphorylation of RNA Polymerase (Pol) I components, which inhibits rDNA transcription. The size and quantity of nucleoli per cell can change dramatically, for example, during differentiation or cancer. However, in general, the "larger the nucleoli, the faster the cell divides," which correlates with greater ribosome biogenesis and growth rates (Villacís *et al.,* 2018*).*

1.5 The process of rRNA transcription

Ribosomal RNA (rRNA) contained within ribosomes is essential for protein synthesis and cellular function in all known species. In eukaryotic cells, rRNA is synthesized from ribosomal DNA clusters of tandem rRNA genes, the organization of which in the nucleolus, maintenance, and transcription are all tightly controlled in order to satisfy the high demand for rRNA required for ribosome biogenesis (Hori *et al.,* 2023).

Most of the ribosome biogenesis occurs in the nucleolus and needs all three RNA polymerases; Pol I and Pol III produce the rRNAs (28S, 18S, 5.8S, 5S) and obligatory processing/modulatory factors, while Pol II generates the various (ribosomal proteins, RPs) and obligatory processing/modulatory factors. Every stage is strictly regulated by signaling

pathways that respond to growth/proliferation, differentiation, and stress stimuli in order to achieve the essential synchronization (Villacis *et al.,* 2018).

The human rRNA transcription unit is 43 kb in size, with 13 kb of pre-rRNA sequences and 30 kb of intergenic spacers where the majority of the rRNA transcription regulatory elements, including the core promoter and the upstream control element (UCE), which are essential cis-acting components that regulate rRNA transcription initiation. The human genome contains several hundred copies of rRNA genes. Transcription of rRNA genes is a highly regulated process that includes initiation, elongation, and termination. The core promoter and the UCE are both required for effective rRNA transcription to begin. The UCE is around 150-200 kb upstream of the rRNA transcription start point and acts as a binding site for the cellular trans-activating proteins involved in RNA polymerase I-mediated transcription. The creation of the pre-initiation complex (PIC) is a critical step in the initiation phase of rRNA gene expression. Transcription of rDNA by Pol I generates a 47S rRNA precursor commencing with the regulated formation of PIC at the promoter and recruitment of RRN3, topoisomerase IIα and the Pol I complex. The recognition of promoters and the creation of PICs rely on synergistic cooperative interactions between UBF and the multi-component SL1 transcription factor complex, which includes the TATA-binding protein (TBP) and TAF factors A-D. It has been demonstrated that the nucleolar-specific HMG-box-containing protein UBF first binds to both the UCE and the core promoter of the rRNA loci, bringing these two DNA elements into proximity and facilitating the association of a hetero-multimeric selectivity factor, TIF-IB, onto the rRNA promoter. The UBF/TIF-IB complex then recruits TIF-IA, which acts as a bridging molecule to bind RNA polymerase I to the rRNA promoter and form a functional PIC for transcription start. After transcription the polymerase is liberated from the PIC and enters the early elongation complex, where RRN3 is released. The transcription of rRNA genes can be controlled at several levels, including post-translational and epigenetic. (Villacis *et al.,* 2018; Tsoi and Chan, 2014).

In addition, the 47S rDNA loci can be identified on the short arms of acrocentric chromosomes (chromosomes 13, 14, 15, 21, and 22 in human cells- Figure 1.5), where they form nucleolus organizer regions. A rDNA is 45 kb long and contains the coding sequence that generates the 47S precursor rRNA, which is then processed into the three mature rRNAs: 18S, 5.8S, and 28S. The 5S and 35S rRNA genes are separated by two intergenic spacers (IGSs), IGS1 and IGS2, which include transcription, replication, and rDNA maintenance regulatory elements. IGS includes retrotransposons and repetitive sequences that account for most of its

length, as well as elements critical for rDNA maintenance such as the RFB (replication fork barrier) site. The RFB site is located at the end of the 47S rRNA gene, and transcription termination factor 1 (TTF1; yeast Reb1 and Nsi1) associates with the 18-bp Sal box sequence in the R repeat. This R repeat is a terminator of the 47S rRNA transcription in the IGS. TTF1 binding to the R repeat, terminates not only rDNA transcription but also the replication fork (Figure 1.5) (Hori *et al.,* 2023; Villacis *et al.,* 2018, Dr Santama's unpublished results).

The rRNA also requires extensive processing, which has only recently been understood in eukaryotes, followed by a series of conformational modifications to allow proteins to bind cooperatively. Factors such as snoRNPs and assembly complexes help in the assembly and maturation of the pre-40S and pre-60S subunits before they are transported to the cytoplasm for the final steps of maturation to a functional ribosome. Intriguingly, ribosome-activity domains such as the peptidyl-transferase domain appear to arise later in the assembly process, presumably to impede translation from immature ribosomes (Villacis *et al.,* 2018).
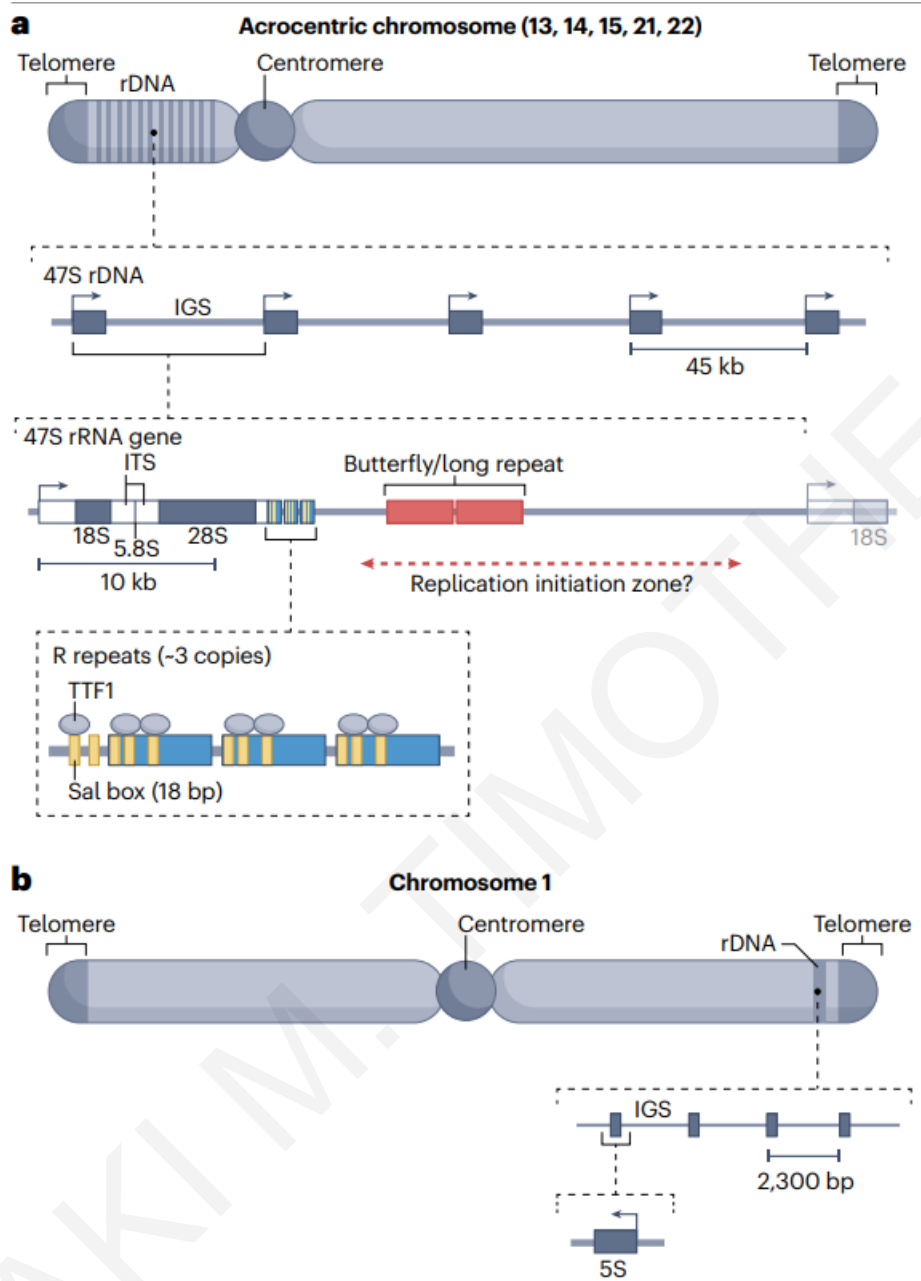
Figure **1.5:**

Organization of the ribosomal rRNA gene in human cells

a) *Human 47S ribosomal RNA (rRNA) genes are structured as clusters on acrocentric chromosomes 13, 14, 15, 21, and 22 and include the 18S, 5.8S, and 28S ribosomal transcripts. Intergenic spacer (IGS) sequences separate the genes, as they do in yeast. TTF1 arrests replication forks by interacting with the Sal box region in the R repeat, which also acts as a terminator of 47S rRNA transcription. The purpose of butterfly/long repeats is unknown. The direction of rRNA gene transcription and ribosomal DNA (rDNA) replication from the replication start zone is indicated by arrows. Human 5S rRNA genes*

b) *The repeat is on chromosome 1. ITS stands for internal transcribed spacer.*

1.6 The aim of this study

One main goal of this study is to quantify rRNA expression and explore the role of KATNAL2 in ribosomal gene transcription. Members of Santama laboratory conducted three independent experiments in wild-type and silenced-KATNAl2 clone-cells cultured in three different serum concentrations of 0.5% (restrictive growth media), 10% (normal growth media), and 20% (enriched growth media) (600 cells in total for WT, 300 cells in total for shKATNAL2 cells clone 2.43 and 300 cells in total for shKATNAL2 cells clone 8-8: that is 100 cells per growth media per cell line). Two distinct sets of wild-type cells were used, each in conjunction with a shKATNAL-2 cell line (WT cells with 2.43 shKATNAL clone cells and WT cells with 8-8 shKATNAL-2 clone cells). As a complement to other approaches, such as Northern blot and quantitative RT-PCR, the cells were briefly incubated with 5-fluorouridine, which is incorporated into nascent RNA as an analogue to uracil, to quantify total rRNA synthesis. The quantitative assessment and statistical evaluation included analysis of FUrd intensity, nucleolar and nuclear size, number of nucleoli, and FUrd intensity/size of the nucleolus. IMARIS software was utilized for analysing microscope images (previously acquired by Ph.D. student Andria Theophanous using a Zeiss Axiovert 200M inverted fluorescence microscope), whereas GraphPad Prism 8 was used for graph display and statistical quantification analysis. The findings reveal that KATNAL2 has an essential role in rRNA transcription, and this is obvious from the nucleolar changes that occurred in the cells upon KATNAL2 silencing.

MATERIALS AND METHODS

2. IMARIS software and its application

The data visualization and analysis tool IMARIS (Interactive Microscopy Image Analysis software) (Bitplane, Oxford Instruments) was used in my study to carry out quantitative analysis of immunofluorescence images acquired with the Zeiss Axiophot 200M inverted microscope. The images utilized were conducted by Ph.D. student Andria Theophanous and became available for my project. The IMARIS software enables the creation of 3D surface illustrations for measurements and quantification for precise data visualization. The entire IMARIS process is thoroughly explained below, with the use of diagrams and images.

2.1. Description and explanation of the IMARIS steps for evaluation of different parameters:

The steps listed below are illustrated in Fig. 2.1 below.

Step 1: The 'Surpass mode' opens images by 'dragging and dropping' them into the IMARIS window.

Step 2: The 'select mode', which is in the top right corner of the IMARIS window, stabilizes the image as opposed to the navigation mode, which moves and rotates the image.

Step 3: The "Surfaces selection tool" is used to select linked objects, surfaces, or volumes in the photos.

Step 4: To create surfaces, the 'skip automatic creation' function can be used before entering the contour and mode.

Step 5: This step depends on the surface to be created. For instance, appropriate buttons would be selected to measure the background, or alternatively, to create a surface in the nucleus or nucleolus.

Step 6: The "draw" button is used to choose the surface of the desired area carefully.

Step 7: Next, the "create surface" button is used to select the surface in order to take various measurements.

Step 8: The 'Statistics' button gathers every parameter measured and generates an Excel file for additional analysis.
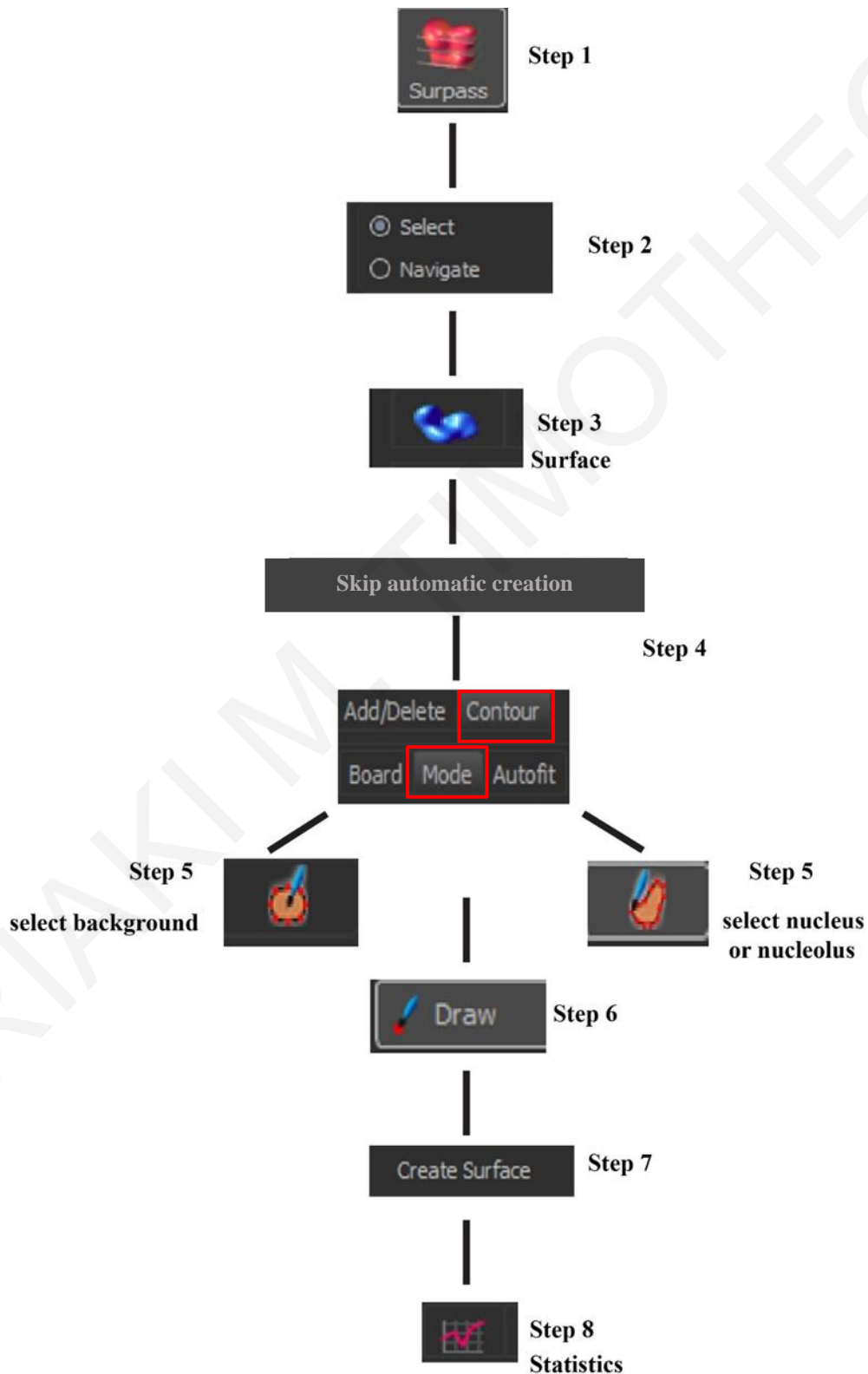
Figure 2.1: Flowchart of IMARIS software

This diagram shows the essential steps to follow on IMARIS software, starting from step one, which uploads the image on the window of the IMARIS, and step two, by picking the 'select' button to make the image stable. The steps between three to eight are used in order to show how to draw and create a surface of the nucleus/nucleoli/ background; the last step gathers all the statistical evaluations and saves them in an Excel file for further analysis.

2.2. Quantitative analysis using IMARIS software

This research focuses on rRNA expression while investigating the function of the KATNAL2 protein in ribosomal gene transcription. To initiate this investigation, scientists from Dr Santama's Laboratory used lentiviral vectors shRNAs that targeted mouse KATNAL2 and transduced the NIH 3T3 fibroblast cell line to generate cells constitutively expressing the KATNAL2 silencing shRNA. To monitor the expression of rRNA, they employed short pulse (15 min) labelling of nascent RNA with FUrd. Three fluorophores were used: the red fluorescence of Alexa 568 to indicates the rRNA expression, the green fluorescence of Alexa 488 for fibrillarin a methyl transferase involved in rRNA processing, and for DNA stained by Hoesch. Two clones, 2,43 shKATNAL2 and 8-8 shKATNAL-2, which displayed the lowest KATNAl2 protein levels, were further analyzed in 3 independent experiments. This analysis was extended to include samples taken at three different growth conditions, with WT and shKATNAL-2 cells cultured to the restrictive growth media (0.5% serum concentration), normal media (10% serum) and enriched growth media (20% serum). There are four datasets that were used to make all the quantifications. The wild-type cells were used in two different periods, each one with the analog shKATNAL-2 cell line. For example, WT cells and 2.43-shKATNAL2 cell lines were used in parallel in three independent experiments (300 cells in total for WT and 300 cells in total for shKATNAL2 cells: 100 cells per growth media per cell line). At another point in time, WT cells and 8-8 shKATNAL2 cells were used in parallel and then cultured to the three different growth medias. (300 cells in total for WT and 300 cells in total for shKATNAL2 cells: 100 cells per growth media per cell line) The quantification analysis was carried out using the IMARIS software.

2.3 Application of the IMARIS software

The nucleus is shown in Fig 2.3 below, along with the red nucleoli that signifies the FUrd incorporation into newly synthesized rRNA. Three fluorophores are seen on the right side of the image: the red fluorescence of Alexa 568, the green fluorescence of Alexa 488 for fibrillarin a methyl transferase involved in rRNA processing, and for DNA stained by Hoescht. In order to monitor the rRNA expression, we chose red. The processes that are depicted in that image by the arrows are the same as in Fig. 2.1.
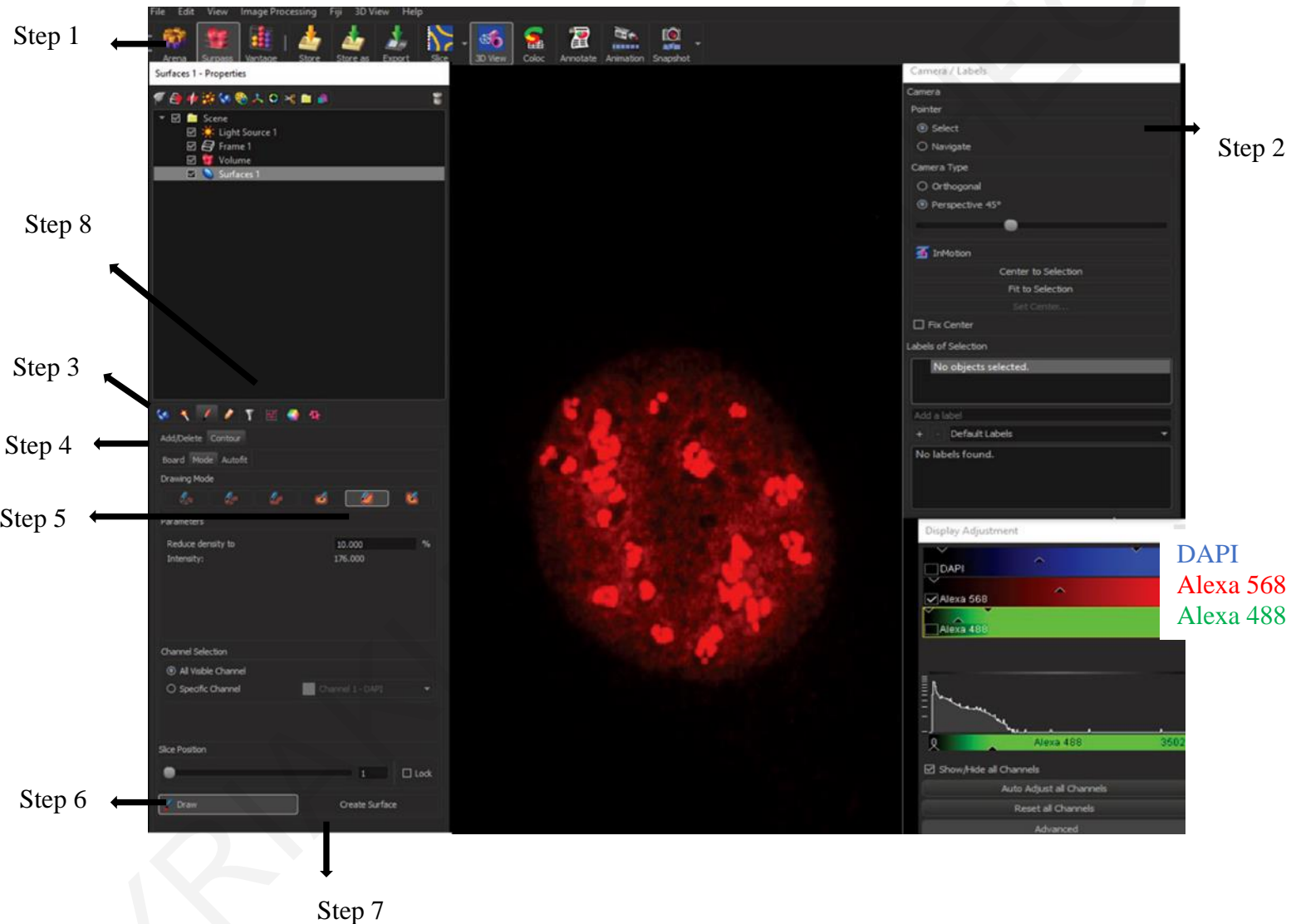
Figure 2.3: Application of the IMARIS software

     Analysis of captured images was performed in each cell from 3 independent experiments using IMARIS software. The image in this representative example shows the nucleus with the nucleoli in red- Alexa 458 indicating the incorporation of the FUrd into the newly synthesized rRNA. Hoescht stained the DNA and fibrillarin with green - Alexa 488 (not shown). The arrows indicate the steps following for IMARIS to evaluate many parameters.

2.4 Selection of surface to quantify the FUrd intensity, the sizes and numbers of nucleoli

     Figure 2.4A shows how each nucleolar surface has been chosen carefully to evaluate the FUrd intensity, the sizes and numbers of nucleoli, and the sizes of the nuclei. Figure 2.4B shows the nucleoli after surface creation (shown in orange). In each case, the measurments are then saved to an Excel file for additional analysis.
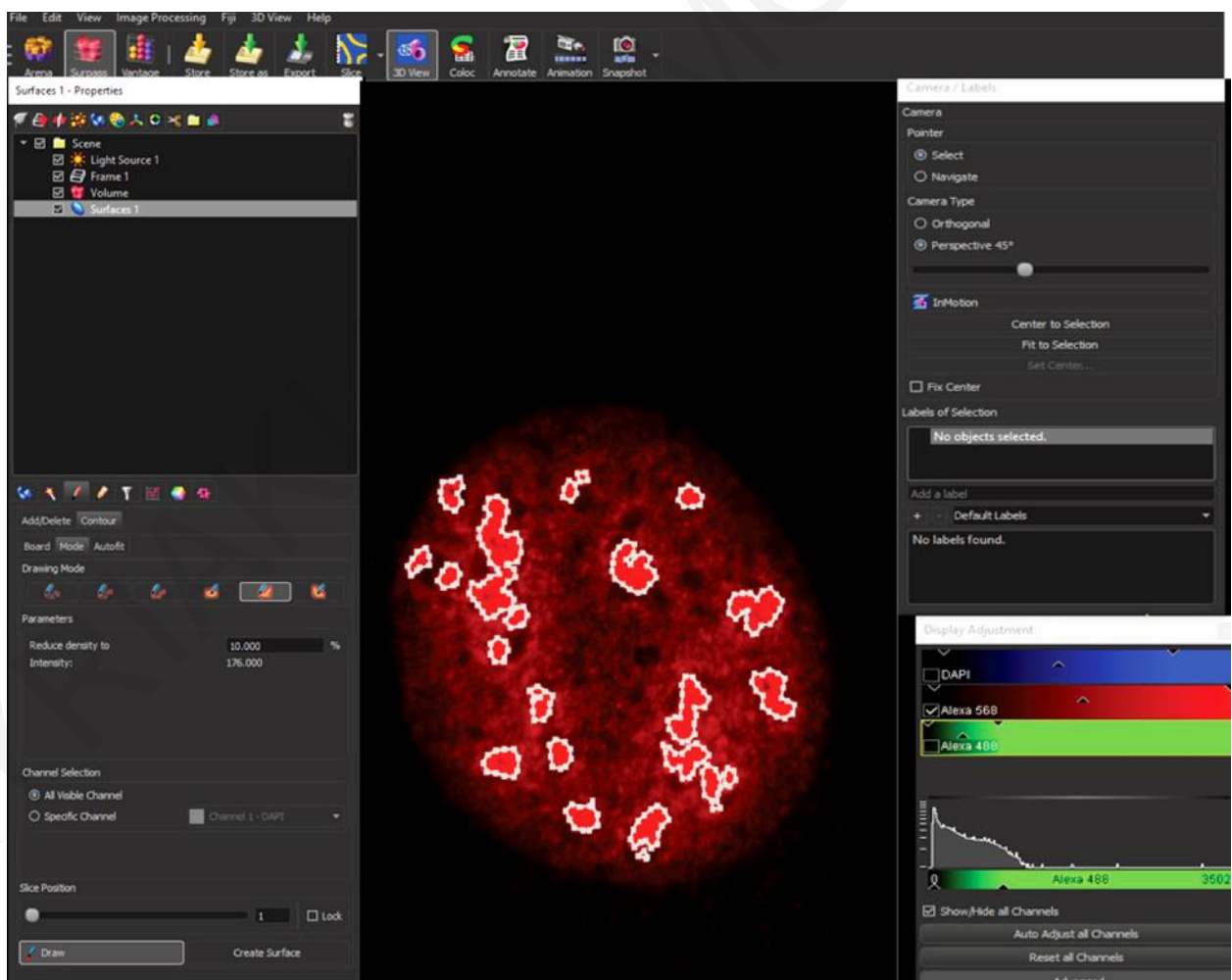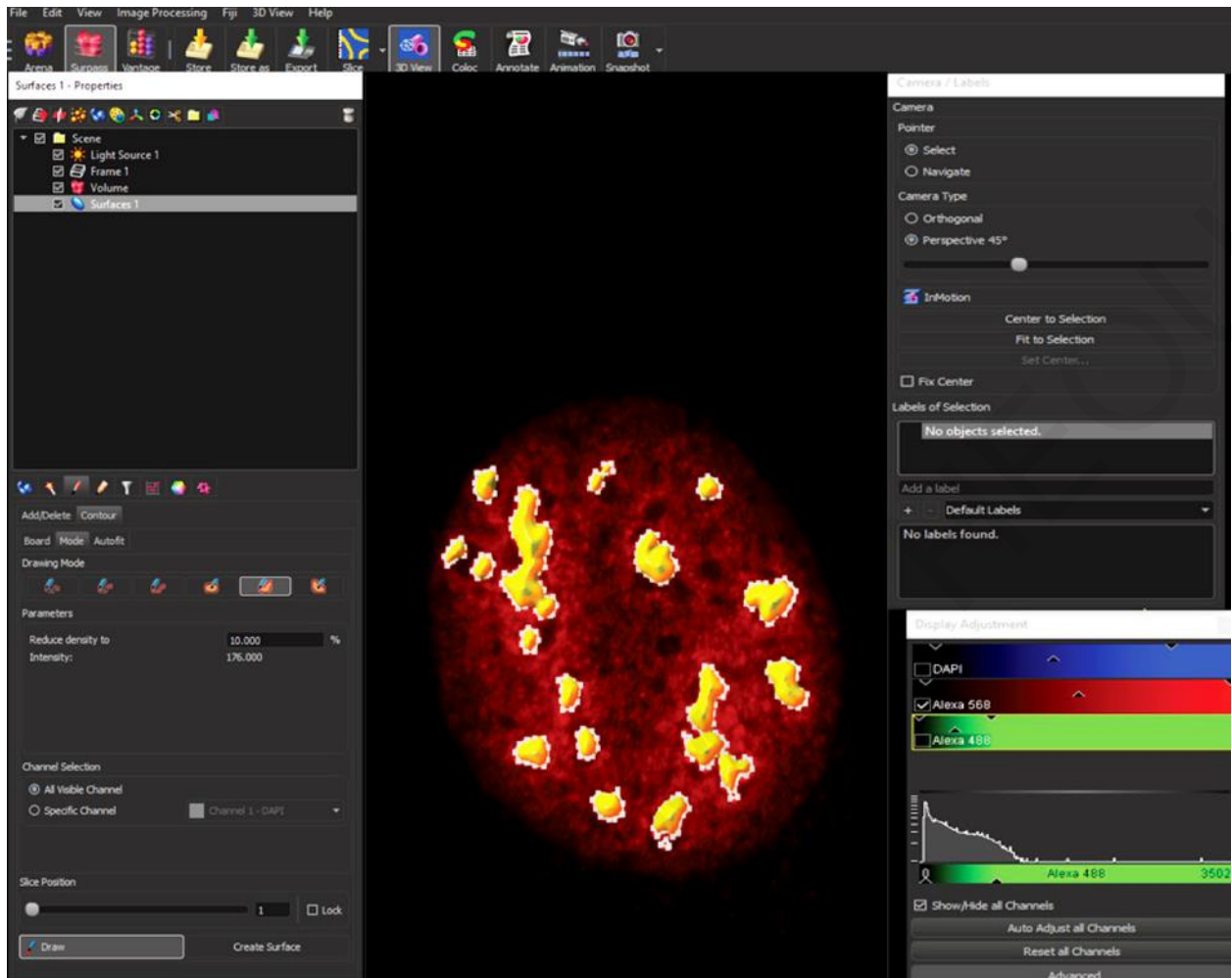
Figures 2.4A and 2.4B: Quantification of FUrd intensity, size and number of nucleoli

Figure 2.4A shows how each nucleolar surface has been chosen carefully by selecting the second button from the end and then pick the draw to choose the surfaces.

Figure 2.4B shows the nucleoli with orange colour after surface creation by selecting the left button 'Create surface'. Each cell's values is saved to an Excel file for further analysis.

2.5 Selection of background

The points have been chosen randomly outside the nucleolus to remove background signals and to make FUrd intensity measurements more representational. Figure 2.5 below, shows the background points approximately 7 to 10 points in the whole nucleus by choosing the 'select background' button on the left.
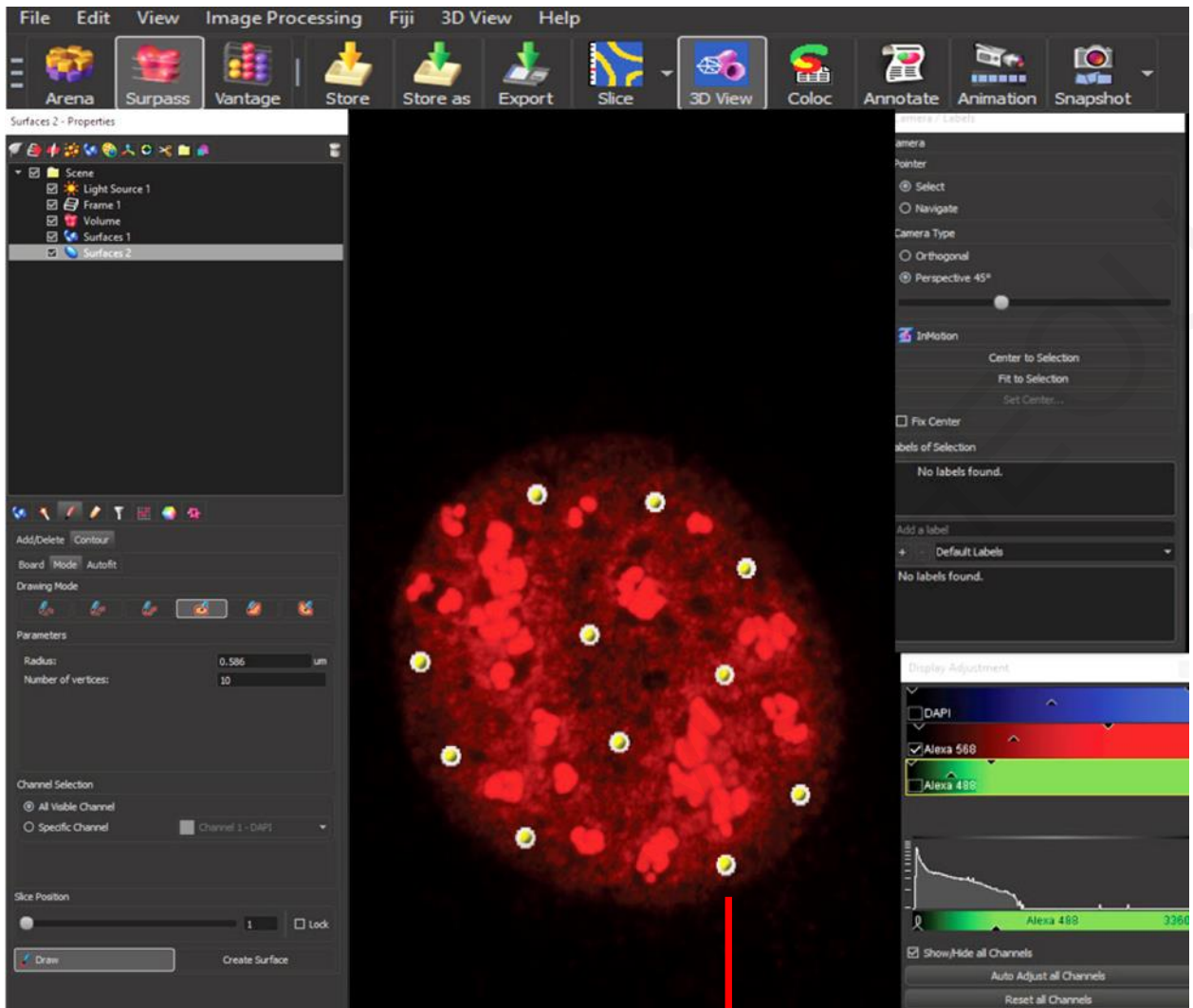
Background points

Figure 2.5: Selection of background

To eliminate background and enhance the assessment of background intensity, the points were chosen at random throughout the entire cell. The backdrop points in the cell are displayed in Figure 2.4 by selecting the 'select background' button on the left.

2.6 Creation of nucleus surface

To investigate whether the nucleus size has changed and in order to compare cell lines and growth medias, the same steps as those for measuring the nucleoli were followed.
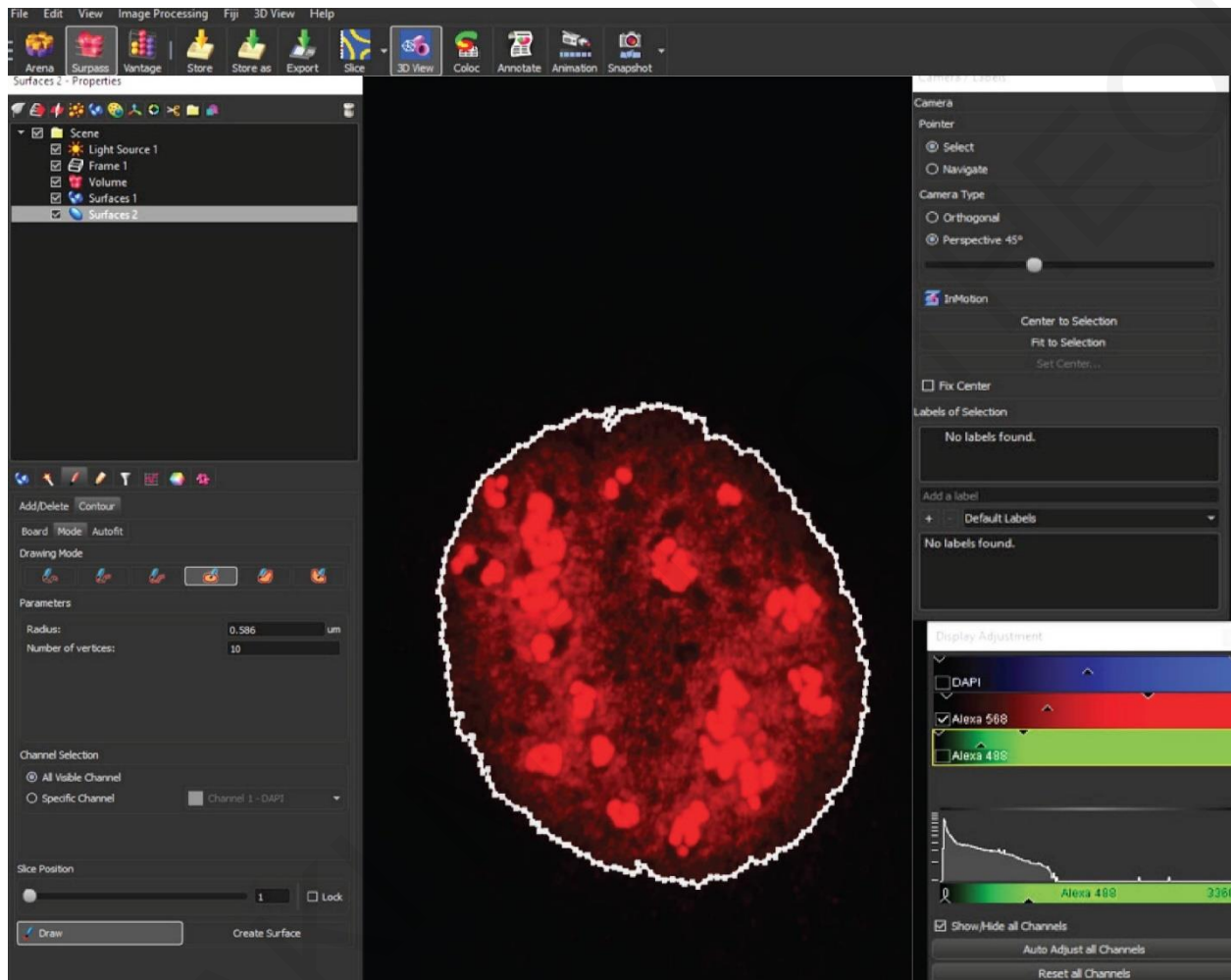
Figure 2.6: Creation of nucleus surface

Following equivalent steps as for the nucleolar size, the size of the nucleus was evaluated to compare among the three experiments and cell lines whether there was a change in the size in different conditions and cell types.

2.7 Evaluation and quantification of statistical analysis

To determine the statistical significance between comparable values, expressed as means or numbers with Standard Deviation (SD) of the three experiments in each cell line conducted in parallel, statistical analyses were carried out using the GraphPad Prism 8.0 Software (GraphPad, Inc.). One-way ANOVA with Tukey's correction or two-way ANOVA with Tukey's correction for differences of one or two variables between more than two groups were used, depending on the circumstances. The two-way ANOVA was used to evaluate the relative mean for the FUrd incorporation and size of the nucleus. On the other hand, the one-way ANOVA was used for statistical evaluation of the size/number of nucleoli and of the FUrd intensity/ nucleolus size. A *p-value* ＜0.05 was regarded as statistically significant (*), <0.01 very significant (**), <0.001 highly significant (***), and <0.0001 extremely significant (****). Any additional statistical analyses used, are mentioned in the figure legends in the Results Chapter.

RESULTS

As already mentioned in the Introduction, the host laboratory contributed the discovery of a new family of KATNAL 2 (Katanin-like 2) in mice. KATNAL2 has been functionally implicated in crucial cellular and developmental processes involving microtubule (MT) remodelling, such as spindle assembly in mitosis, ciliogenesis and neuronal morphogenesis (Ververis *et al*., 2016; Willsey 2018). More precisely, the investigation of KATNAL 2 has been extended in vertebrate embryonic development since the absence of katnal2 expression revealed that in the *Xenopus tropicalis* embryo/tadpole, the CRISPR gene editing or morpholinos for Katnal2 had marked effects on neurogenesis, affecting proper blastopore closure, neural tube closure and inhibiting neural crest cell migration (Willsey *et al*., 2018). Unexpectedly, despite the intracellular localization of KATNAL 2 in MTs, a fraction of KATNAL2 resides in the nucleolus. Therefore, Santama Laboratory members investigated further KATNAL 2 in the nucleolus (unpublished).

After a series of experiments that have been conducted, it was observed that in nucleoli of mouse NIH 3T3 cells (and other cell lines), KATNAL2 is localized nearby, almost overlapping with the rRNA transcriptional activator UBF and rRNA methyltransferase fibrillarin, proteins that are markers of the Fibrillar Component (FC) and the Dense Fibrillar Center (DFC) of the nucleolus, respectively. Additionally, nucleolar proteins UBF, fibrillarin, treacle, and RNA Pol. I, a portion of KATNAL2 was enriched in the chromatin fraction, indicating that KATNAL2 is bound to chromosomal DNA (unpublished).

Additional RNA metabolic labelling experiments were conducted by comparing cells of the wild-type and KATNAL2-silenced in order to quantify the pre-rRNA and major processing rRNA species. Quantitative analysis of the 47S rRNA and major rRNA species was carried out to evaluate rRNA processing because initial analysis with Northern blots suggested potential rRNA processing problems in the absence of KATNAL2 (unpublished results).

The primary purpose of this study is to monitor the expression of the rRNA and to study the role of KATNAL2 in ribosomal gene transcription. To achieve that, members of the Santama's laboratory performed three independent experiments using wild-type and KATNAL2-silenced cells, cultured in three different serum concentrations of 0.5% (restrictive growth media), 10% (normal growth media) and 20% (enriched growth media) (n=100 per condition and cell line). As a complement to other approaches, such as Northern blot and quantitative RT-PCR, the cells were incubated shortly with 5-fluorouridine, incorporated into

a nascent RNA as an analogue to uracil, to assess total rRNA production. In this thesis, the quantitative analysis and statistical evaluation of these experiments was conducted studying the following parameters: FUrd intensity, the nucleolar and nuclear size, the number of nucleoli, FUrd intensity/size of the nucleolus. The IMARIS software was used to analyze microscope-captured pictures, and GraphPad Prism 8 was used for graph presentation and statistical analysis of quantifications. This chapter presents an overview of the study's results.

3.1 Quantitative analysis of FUrd intensity after its incorporation into the newly synthesized RNA in the nucleolus

One of the approaches employed in this study was the incorporation FUrd into nascent RNA by short pulse labeling; the quantification of the mean fluorescence intensity in the nucleoli of many cells was used as a proxy in order to monitor rRNA expression, Figure 3.1 illustrates that the WT and shKATNAL-2 cells grew in three different growth media: restrictive (0.5% serum concentration), normal (10% serum concentration), and enriched (20% serum concentration) growth media. The immunofluorescence images in Figure 3.1 show that the FUrd incorporation was marked red (Fig 3.1 A, D and G), DNA was stained with Hoechst (Fig. 3.1 B, E and H), and the last images show the overlay of the two colours (Fig.3.1 C, F and I). With serum concentration increasing from 0.5% to 20%, we can significantly observe an increase of FUrd intensity in shKATNAL-2 cells, relative to WT cells, at every serum concentration.

More specifically, quantitative, and statistical analysis is presented with graphs and Tables for this experiment. Fig. 3.2 graph A (results summarized in Table 3.1) compares FUrd intensity between the WT cells and the sh2.43 shKATNAL-2 clone cells. It shows the increase of FUrd incorporation in the shKATNAL-2 cells compared to the WT cells at every serum concentration (Figure 3.2 A). A higher than a 2-fold increase is observed in the 0.5% and 10% serum growth media in shKATNAL-2 cells relative to WT (p-value 0.0064 and p- value <0.0001, respectively) and a 1.72-fold increase at 20% serum (p-value<0.0001).
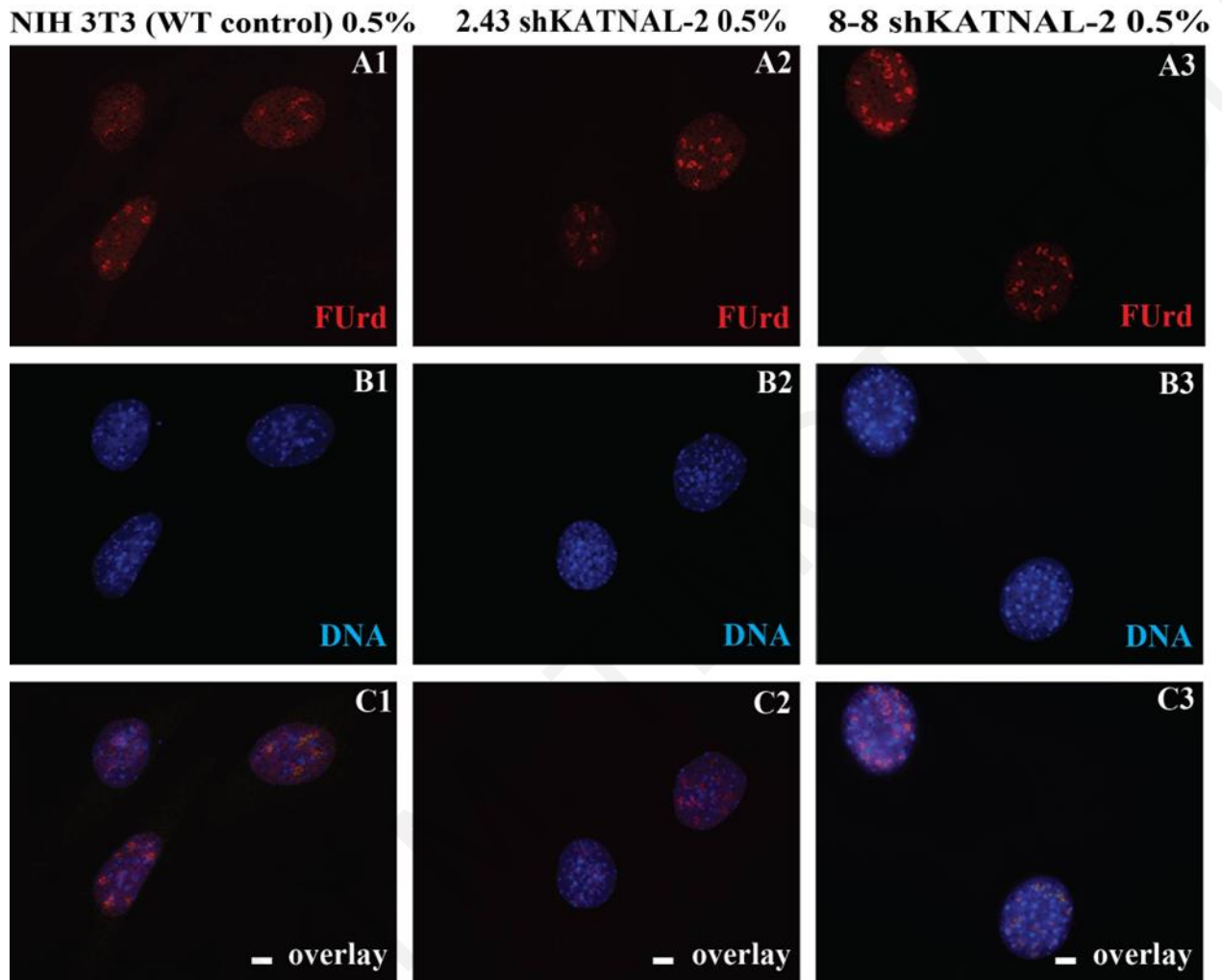
Similarly, the same pattern is shown in Fig.3 B and Table 3.2, which compare the WT cells and the 8-8 shKATNAL-2 clone cells. In this case, the comparisons reveal more modest difference than those observed for 2.43: in particular no increase is observed at 0.5% while at

10% serum growth media there is a 0.62-fold increase in FUrd incorporation in shKATNAL-2 cells relative to WT (p-value <0.0001 and a 0.7-fold increase at 20% serum (p-value 0.0007).

Therefore, cells that are exposed to the restrictive growth media (0.5% serum concentration) express less rRNA because of the decrease in growth factors in relation to the enriched growth media (20% serum concentration), in which the cells are exposed to more growth factors, thus, express more rRNA. The two tables represent the means and the standard deviation (±SD) for every cell for all three experiments individually in order to make the differences between them more apparent. In statistics, the standard deviation is a measure of the amount of variation or dispersion of a set of values. A low standard deviation indicates that the values tend to be close to the mean of the set, while a high standard deviation indicates that the values are spread out over a wider range. In the case of FUrd intensity, the means seem to be following an upward trend whenever the serum concentration rises in all three cell lines but in the shKATNAL-2 clone cells there is a significant increase in comparison with the WT. Between the means of clone cells, the 2.43 cells are slightly elevated. Overall, it is observed that the two clones named 2.43 shKATNAL-2 and 8-8 shKATNAL-2 have a noticeable increase in the FUrd intensity as well as in rRNA expression with the absence of KATNAL 2 compared in WT, which leads to the suggestion that the KATNAL 2 plays an essential role to the transcription of RNA.
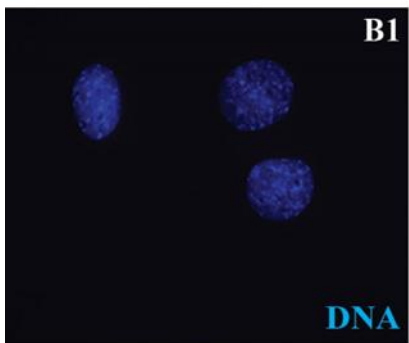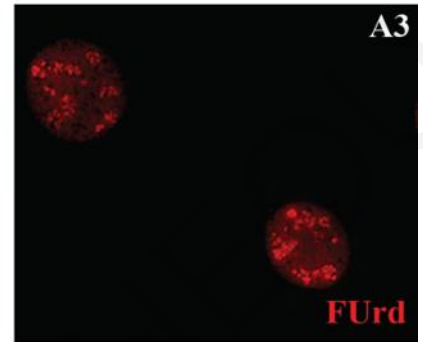
Figure 3.1

FUrd Intensity

NIH 3T3 (WT control) 0.5%	2.43 shKATNAL-2 0.5%	8-8 shKATNAL-2 0.5%

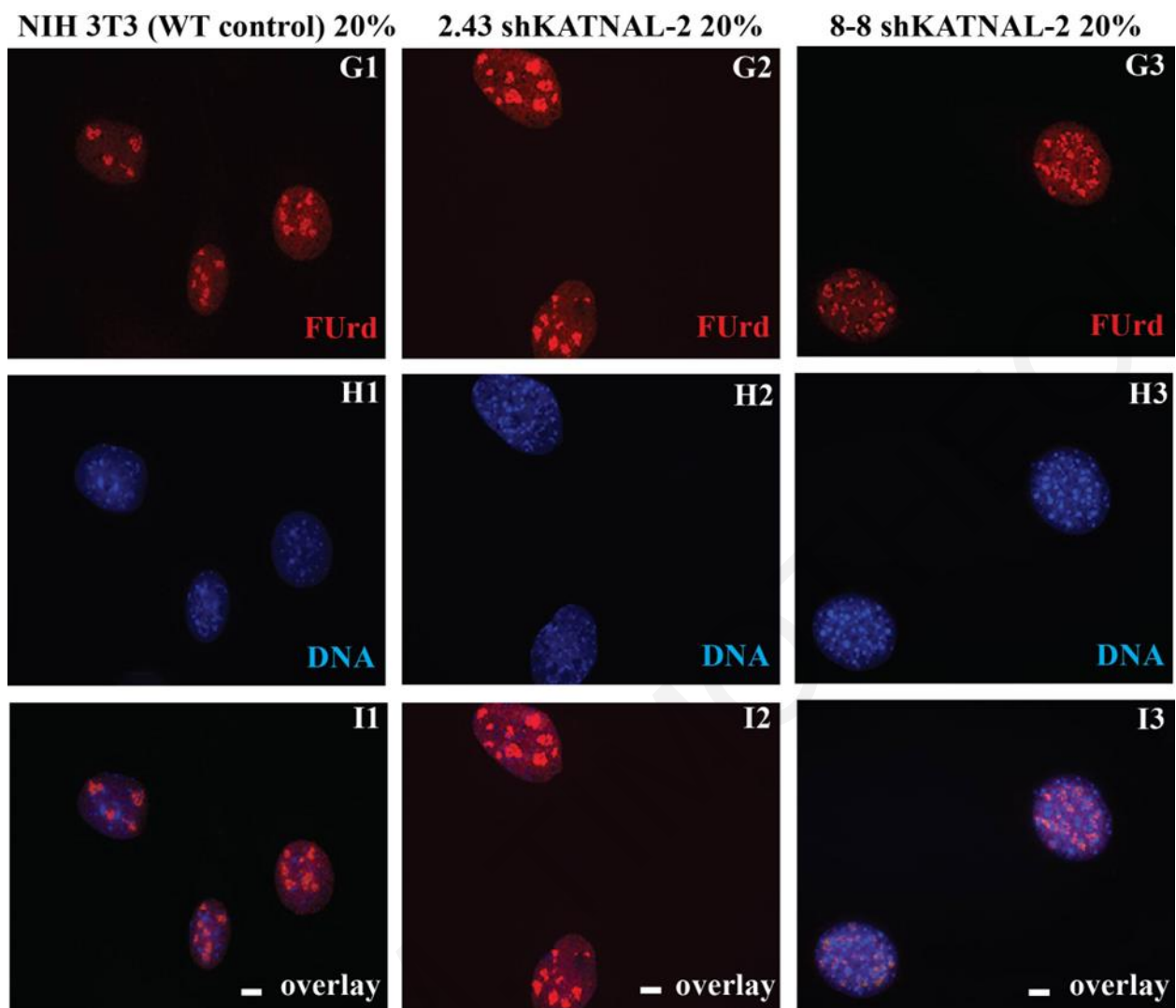| NIH 3T3 (WT control) 10%	2.43 shKATNAL-2 10%	8-8 shKATNAL-2 10%
A1 FUrd	A2 FUrd	A3 FUrd
B1 DNA	B2 DNA	B3 DNA
C1 overlay	C2 overlay	C3 overlay
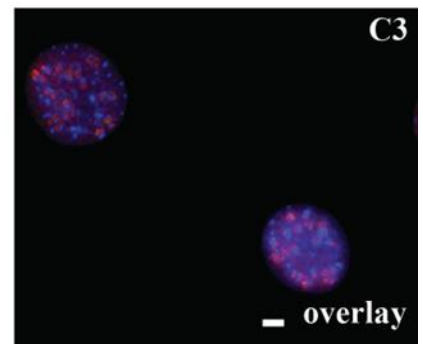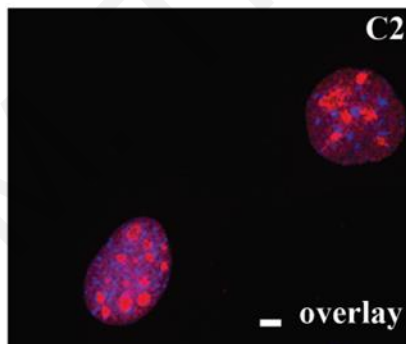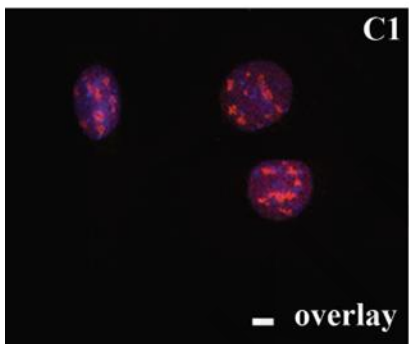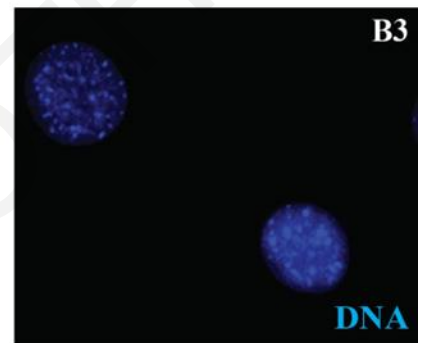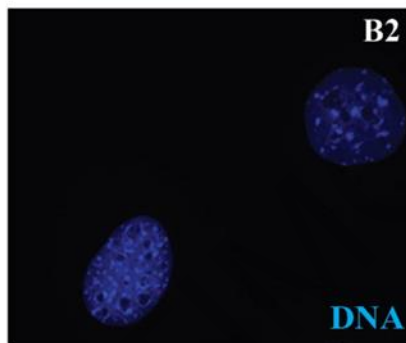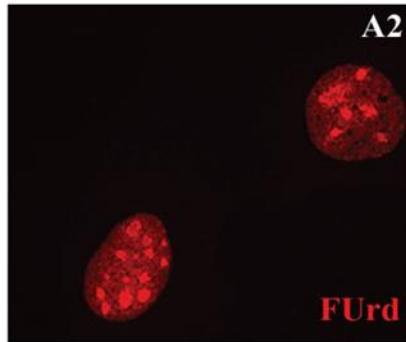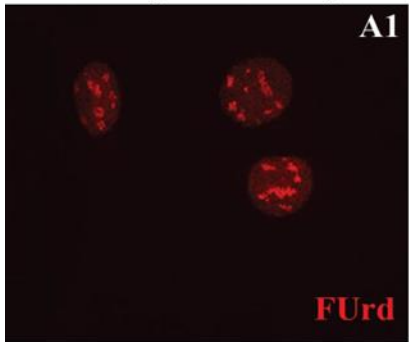
Figure 3.1: Illustration of FUrd intensity after incorporation into the newly synthesized RNA

(A1-I3) Representative immunofluorescence images of cells cultured in three independent growth media: restrictive growth media (0.5% serum concentration), normal growth media (10%) and enriched growth media (20%). The first horizontal red images indicate the incorporation of FUrd into the nascent RNA. The images with blue correspond to the DNA stained by Hoechst and the overlay of the two colours is also shown. Scale bar is 10μm.

(A, D, G): *There is a visible increase in the FUrd intensity and, therefore, in the expression of rRNA in shKATNAL-2 cells at all growth media, relative to WT cells. The increase is evident with the bright red colour observed in the 10% and 20% serum concentrations in contrast to the 0.5% serum concentration in all the cell lines. In shKATNAL-2 cells, present a significant increase of FUrd intensity, mainly in 20% serum concentration compared to WT cells.*

36

Figure 3.2 A and B

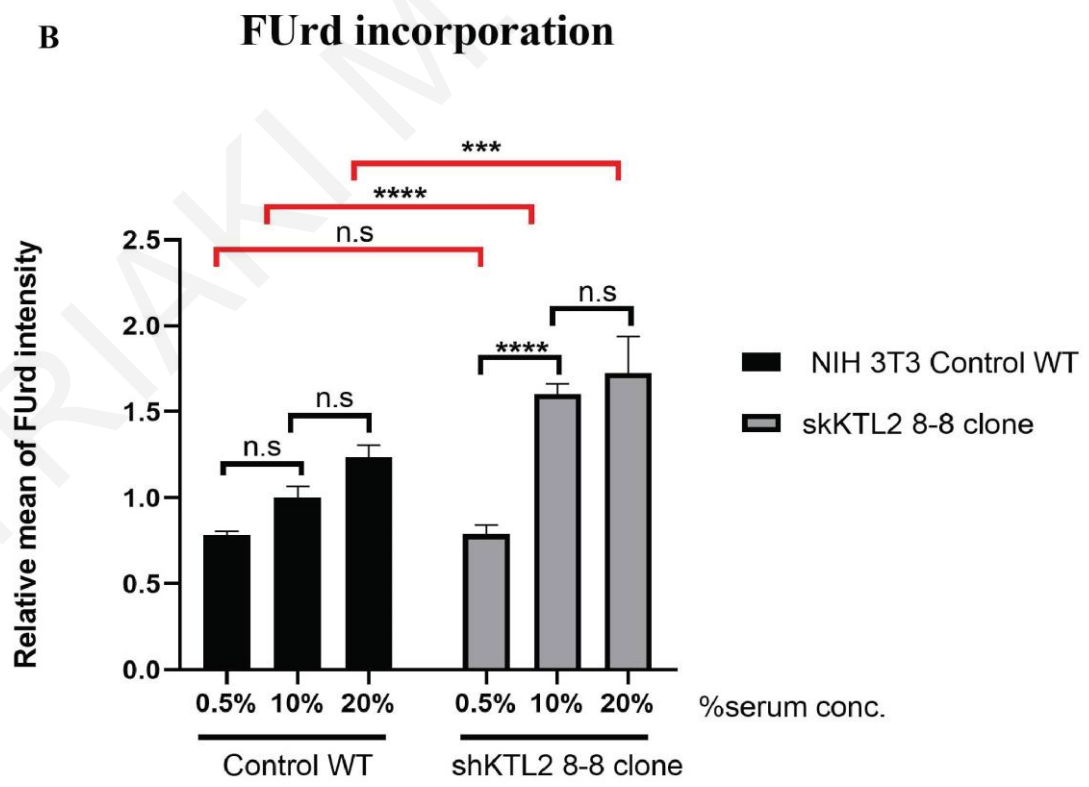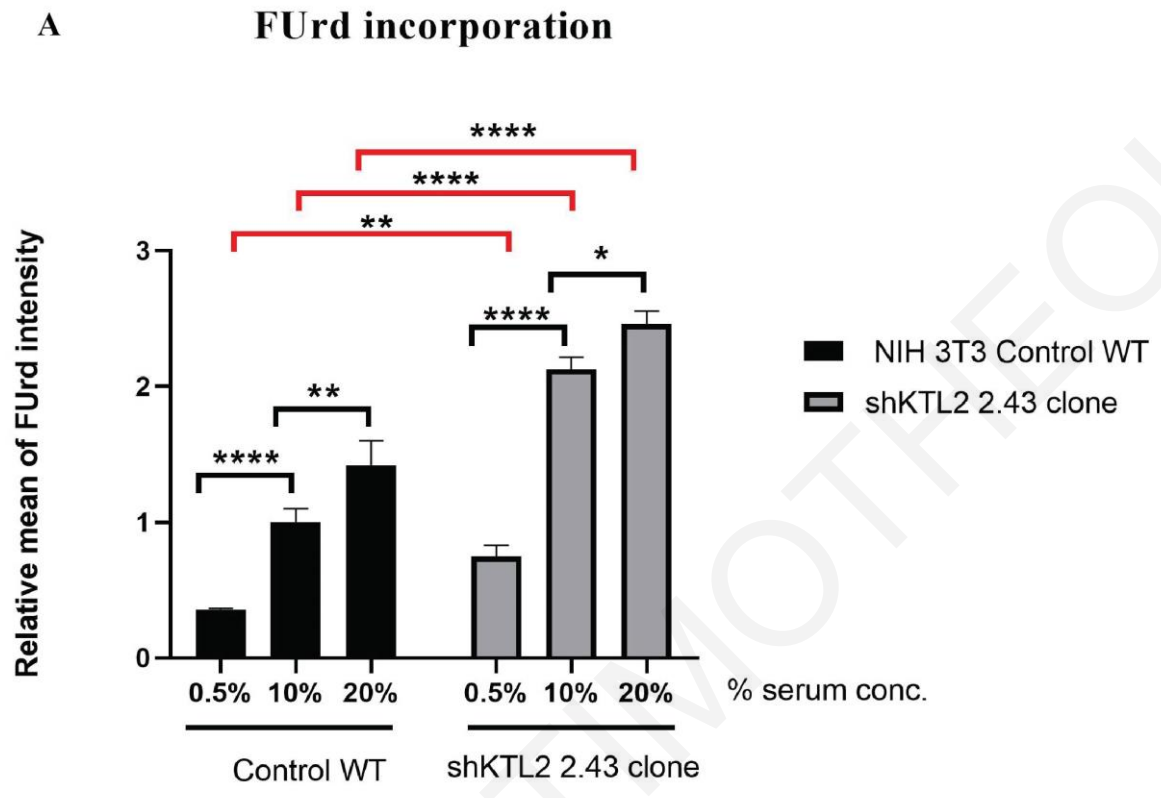A   FUrd incorporation

B   FUrd incorporation

Figure 3.2 A+B: Quantification of FUrd incorporation into newly transcribed RNA in the nucleolus

Quantifying relative FUrd incorporation into newly transcribed RNA in the nucleolus in the same experimental setup as in Fig. 3.1.

A) *Graph A compares WT cells and 2.43 shKATNAL-2 clone cells in the mean FUrd intensity of the cells cultured in three different growth media. There is an upward trend of increase of FUrd incorporation in line with serum concentration increase between the three experiments in both cell lines. And a significant increase of mean FUrd incorporation in shKATNAL-2 relative to WT cells, at all growth conditions.*

B) *Graph B illustrates the differences in the FUrd intensity between the WT and 8-8 shKATNAL-2 clone cells. Compared to WT, there is an increase in the FUrd in the shKATNAL-2 8-8 clone only at 10 and 20% serum, compared to WT cells.*

Two-way ANOVA with Tukey's correction assessed the statistical significance of differences. A p-value $<$ 0.05 regarded as statistically significant (*), <0.01 very significant (**), <0.001 highly significant (***), and <0.0001 extremely significant (****).

Table 3.1: Representative mean and standard deviation values between WT and 2.43 shKATNAL-2 cells after the FUrd incorporation into nascent RNA					
NIH 3T3 (WT control)			**2.43 shKATNAL-2**		
	0.5% serum conc.	**10% serum conc.**	**20% serum conc.**	**0.5% serum conc.**	**10% serum conc**	**20% serum conc.**
mean	0.35409326	1	1.42098623	0.74622498	2.12639144	2.45648015
± SD	0.0099805	0.10104257	0.17755609	0.08318686	0.08618497	0.09838238

Table 3.2: Representative mean and standard deviation values between WT and 8-8 shKATNAL-2 cells after the FUrd incorporation into nascent RNA					
NIH 3T3 (WT control)			**8-8 shKATNAL-2**		
	0.5% serum conc.	**10% serum conc.**	**20% serum conc.**	**0.5% serum conc.**	**10% serum conc**	**20% serum conc.**
mean	0.781624236	1	1.236391475	0.788042749	1.603697491	1.726041468
± SD	0.0099805	0.10104257	0.17755609	0.054446063	0.058439467	0.210983783

3.2 Silencing of KATNAl 2 causes increase in the size of the nucleoli

It is known that the nucleolus acts as a sensor of cellular stress and alters its structure morphologically and molecularly in response. An increase in protein synthesis and growth is indicated by an increase in the nucleolar size (Hariharan and Sussman, 2013).

According to the findings from members of Santama's laboratory, there are morphological changes in the structure of the nucleoli upon KATNAL2 silencing. Specifically, nucleoli were enlarged in comparison with the wild type. Additional analysis by Electron Microscopy confirmed the modifications in the fine structure of nucleoli. It revealed that the dense fibrillar component (DFC) was expanded at the expense of the fibrillar centre (FC) (unpublished results).

After successfully incorporating FUrd into the newly synthesized RNA, and as the expression of RNA in shKATNAL2 cells increases, we hypothesized that the size of the nucleoli might change. The conditions and the cell lines are in the same experimental setup, so we estimated the size of each nucleolus per growth media and cell line (0.5%, 10% and 20% serum concentration) using the IMARIS software.

There is an upward trend regarding the nucleoli size between the three growth media in the both WT and KATNAL2-silenced cell lines with the 20% serum concentrations show the largest sizes of the nucleoli (Fig. 3.3). However, the shKATNAL-2 cell lines illustrated a visible increase in nucleoli sizes compared to WT. The images in Figure 3.3 shown with red colour the

expression of RNA into the nucleolus; the DNA is shown blue due to being stained by Hoechst, and the third line represents the overlay of the two colours (Fig 3.3, A, D, G).

Comparing the two graphs that illustrate the quantification of mean differences in nucleoli sizes between WT cells since the 2.43 shKATNAL-2 clone cells and 8-8 shKATNAL-2 clone cells (Fig. 3.4 A and B, respectively, Tables 3.3. and 3.4). It is worth mentioning that in 2.43 shKATNAL2 cells the mean values are significant increase compared to WT. The enriched growth media shows the larger sizes of nucleoli a slightly over 150 μm and with mean value 27 for the shKATNAL-2 clone cells compared to WT that have mean 21.22 (p-value is <0.0001). At the same time, in restrictive and normal growth media, the larger sizes reached up to 100μm in WT cells (p-value <0.0001) with mean 13.69 and 16.16 respectively. Identically, shKATNAL-2 cells in a restrictive growth media reached up to 100μm, and it has a remarkable increase in the mean with 17.87 compared to WT. Despite this, shKATNAL-2 cells in the normal growth media indicated sizes between 100 to 150 and the mean value is 18.52, which is higher than in WT cells.

The results with shKATNAL2 8-8 silenced cells (Fig. 3.4 B, Table 3.4) are similar, however, in WT cells the maximum sizes are close to 100μm for restrictive and normal growth media. The mean value in WT is 15.06 for 0.5% serum, compared to the 0.5% serum in shKATNAL2 cells that have mean 15.48. The normal and enriched growth media in 8-8 shKATNAL-2 cells are similar to the respectively growth media in graph A but the mean and SD values are slightly increased in the 2.43 shKATNAL-2 cells rather than the 8-8 shKATNAL-2 cells except in 10% serum of 2.43 clone that is negligible decreased from the 10% serum of 8-8 shKATNAL-2 cells. For example, in 8-8 shKATNAL2 the mean values for 10% and 20% sera are 17.08 and 22.26 respectively.

The typical size of a nucleolus varies between 0.2-3.5 micron; therefore, the cells enlarge their nucleoli due to increased RNA expression. To sum up, we can suggest that the more RNA production we have, the larger the nucleoli, this is more conspicuous in the silenced-KATNAL-2 cells.
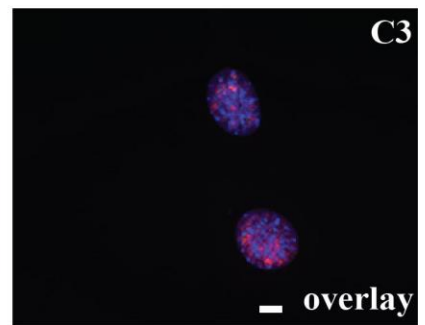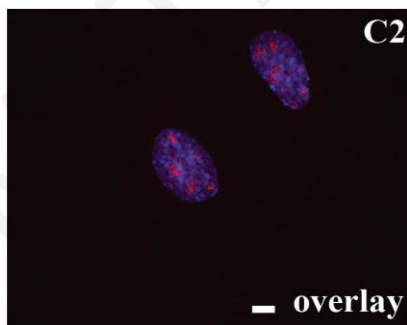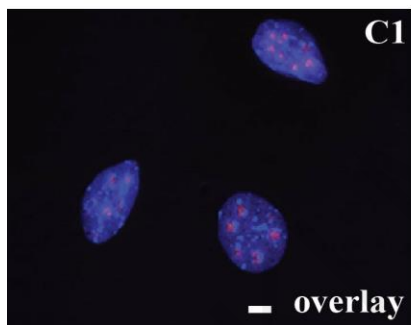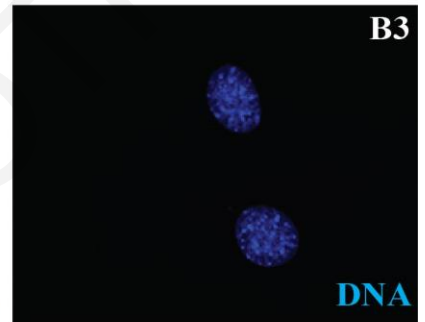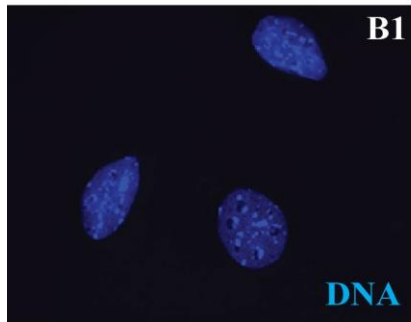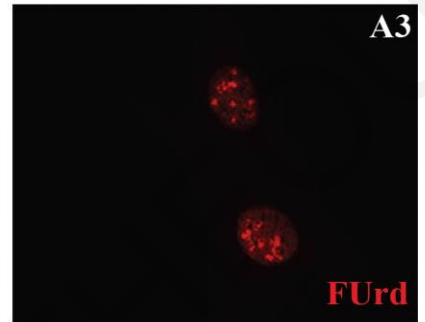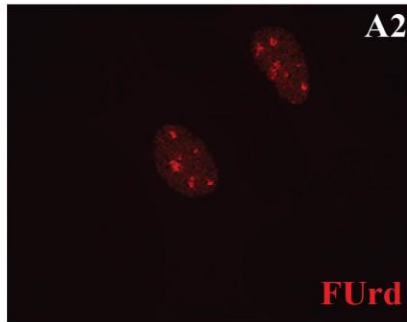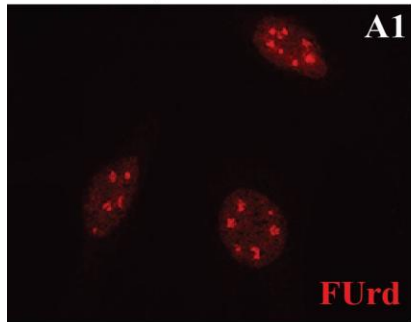
Figure 3.3

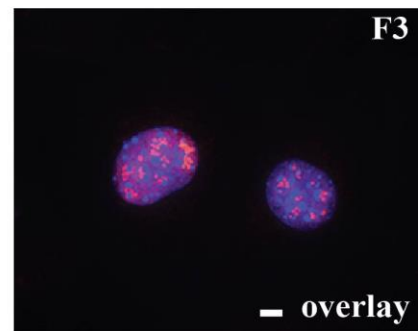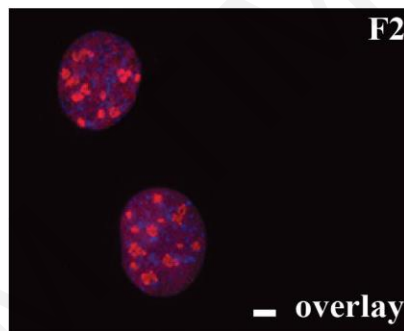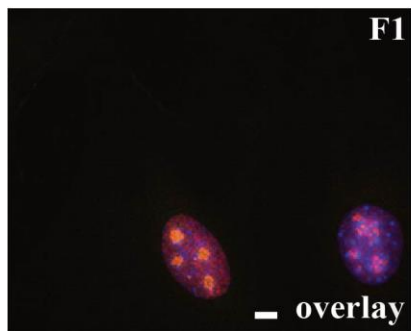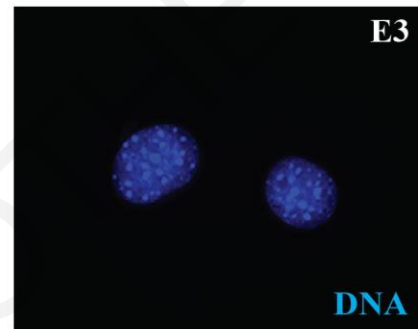## Nucleoli sizes

NIH 3T3 (WT control) 0.5%	2.43 shKATNAL-2 0.5%	8-8 shKATNAL-2 0.5%

NIH 3T3 (WT control) 10% 2.43 shKATNAL-2 10% 8-8 shKATNAL-2 10%

D1 FUrd D2 FUrd D3 FUrd
E1 DNA E2 DNA E3 DNA
F1 overlay F2 overlay F3 overlay
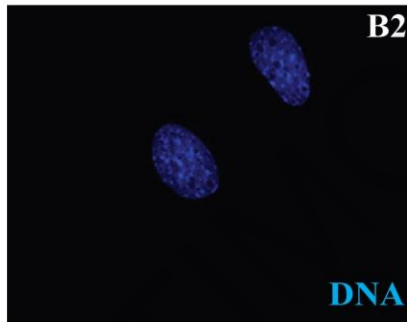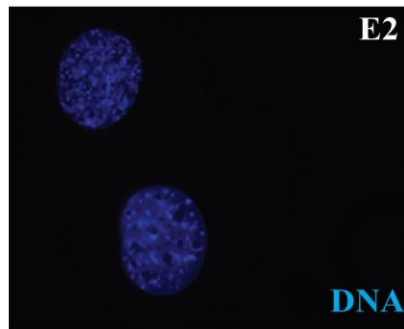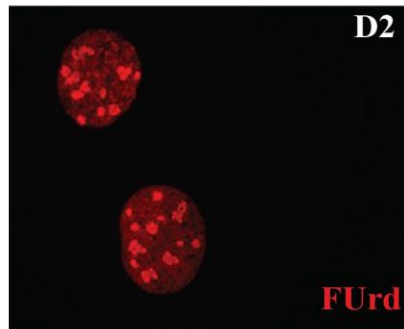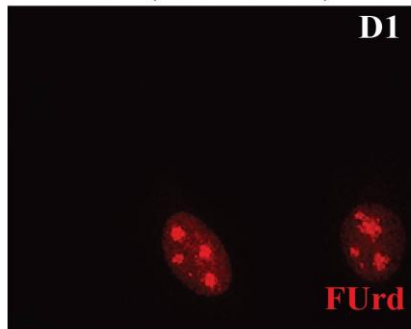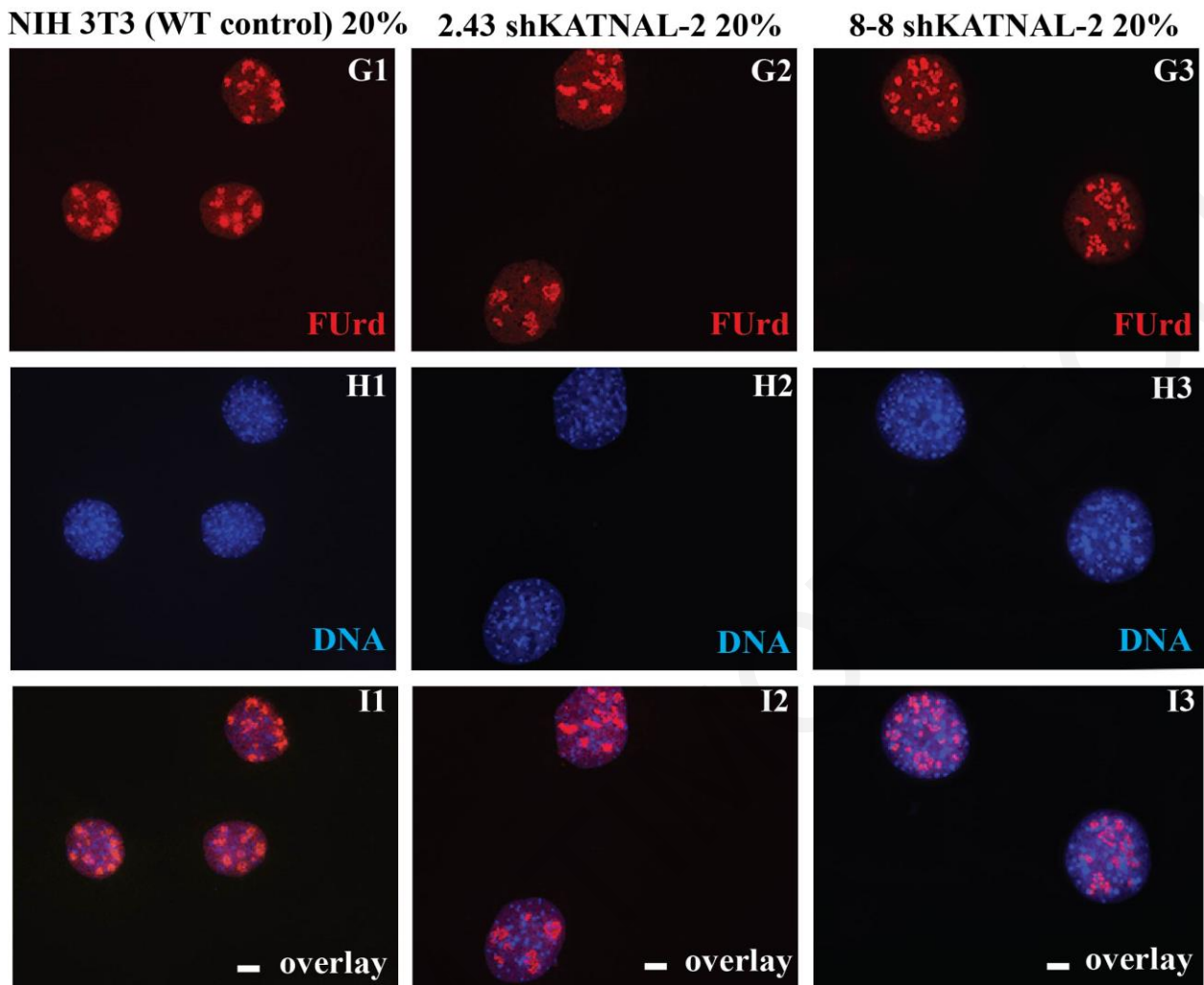
Figure 3.3 Illustration of increase in the size of nucleoli upon silencing of KATNAL- 2.

(A1-I3) Observation and evaluation of relative nucleoli size. Representative immunofluorescence images of cells cultured in three independent growth media: restrictive growth media (0.5% serum concentration), normal growth media (10%) and enriched growth media (20%). The first horizontal red images indicate the incorporation of FUrd into the n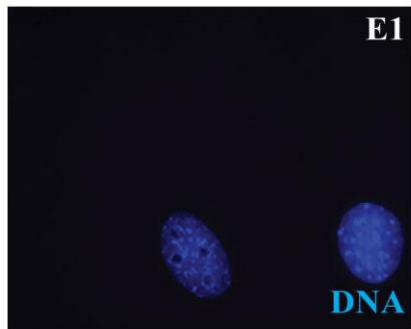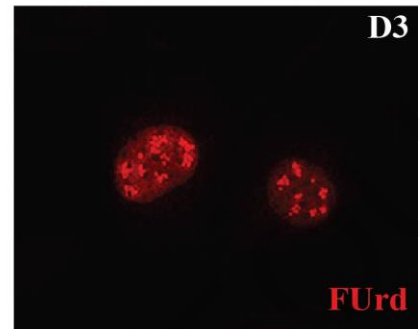ascent RNA, while the images with blue correspond to the DNA stained by Hoechst and the overlay of the two colours is also shown. Scale bar is 10μm.

(A, D, G) The images represent the change in nucleoli size for each cell line and in serum concentration. It is observed that an upward trend in the nucleoli size in all cell lines. However, the shKATNAL-2 cells show larger nucleoli compared to WT. Also, there is a difference in nucleoli size between the three growth media (0.5%, 10% and 20% serum concentrations). For instance, the enriched growth media (20% serum concentration) has the largest nucleoli in all cell lines than the other two growth media.

A

Nucleolar size

Relative nucleolar size (y-axis)

Categories: NIH 3T3 0.5%, NIH 3T3 10%, NIH 3T3 20%, shKTL2 2.43 clone 0.5%, shKTL2 2.43 clone 10%, shKTL2 2.43 clone 20%

serum concentration

B

Nucleolar size

Relative nucleolar size (y-axis)

Categories: NIH 3T3 0.5%, NIH 3T3 10%, NIH 3T3 20%, shKTL 2 8-8 clone 0.5%, shKTL 2 8-8 cone 10%, shKTL 2 8-8 clone 20%
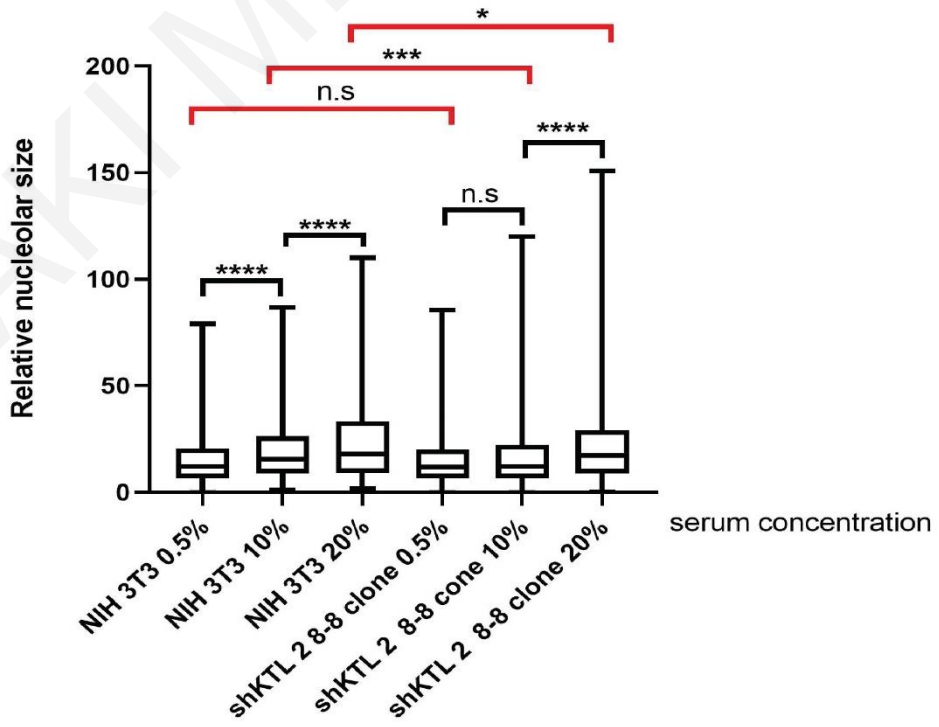
serum concentration

44
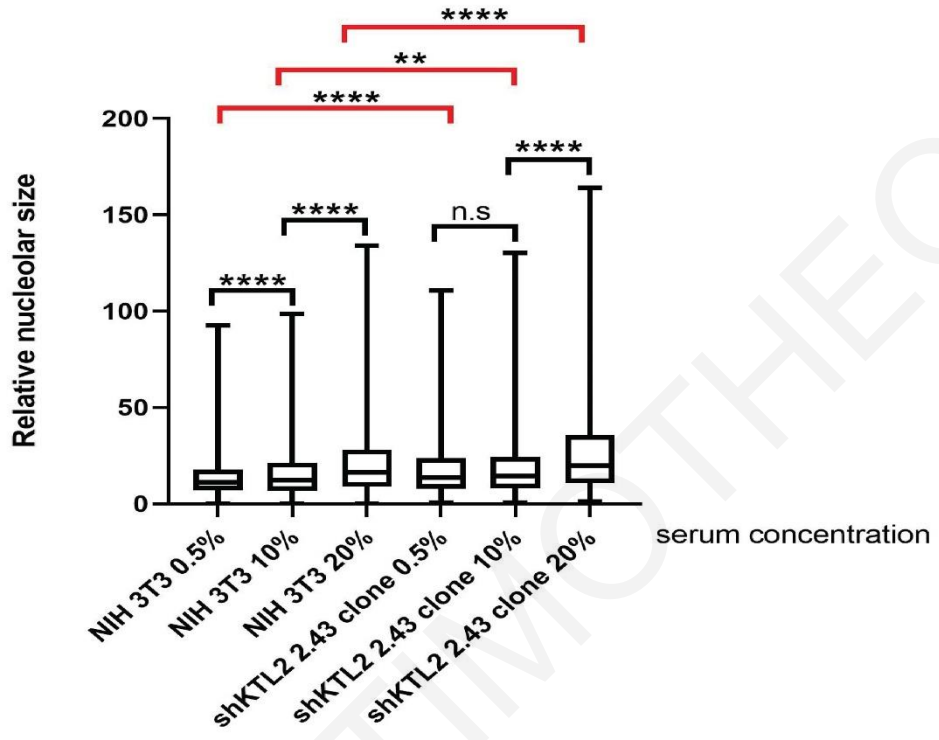
Figure 3.4 Quantification and statistical analysis of the nucleoli size

Graphs A and B: *Presentation of measured nucleoli sizes in all cell lines and growth media. There is an increase in the nucleoli size among the growth media in both graphs, with the enriched growth media enlarging nucleoli more than the other two media. Also, again the shKATNAL-2 cells present a rise in the nucleoli size compared to WT, maybe the absence of KATNAL 2 contributes to more RNA expression, thus increasing the nucleoli size.*

One-way ANOVA assessed the statistical significance of differences with Tukey's correction. A p-value <0.05 is regarded as statistically significant (*), <0.01 very significant (**), <0.001 highly significant (***), and <0.0001 extremely significant (****).

Table 3.3: Differences in mean and standard deviation values in WT and 2.43 shKATNAL-2 cells to compare the size of the nucleoli					
NIH 3T3 (WT control)			**2.43 shKATNAL-2**		
	0.5% serum conc.	**10% serum conc.**	**20% serum conc.**	**0.5% serum conc.**	**10% serum conc**	**20% serum conc.**
Mean	13.79	16.16	21.22	17.87	18.52	27.00
± SD	10.25	13.48	17.58	14.00	15.13	23.22

Table 3.4: Differences in mean and standard deviation values in WT and 8-8 shKATNAL-2 cells to compare the size of the nucleoli					
NIH 3T3 (WT control)			**8-8 shKATNAL-2**		
	0.5% serum conc.	**10% serum conc.**	**20% serum conc.**	**0.5% serum conc.**	**10% serum conc**	**20% serum conc.**
Mean	15.06	20.03	24.13	15.48	17.08	22.26
± SD	11.39	15.40	19.60	12.51	15.25	18.87

3.3 Distribution of the FUrd intensity in the various sizes of the nucleoli between WT cells and shKATNAL-2 cells

Following the measuring of FUrd intensity and nucleolus size individually, which are presented as increased in silenced-KATNAL2 clones compared to wild-type cells, we would like to find out if nucleolus size plays an essential role in the increased RNA transcription. Quantification of FUrd mean intensity normalized per the corresponding nucleolar size showed that the shKATNAL-2 cells presented increased intensity per nucleolus, demonstrating the increase of RNA expression per unit area of the nucleolus in relation to WT cells. We used the IMARIS software to quantify FUrd intensity for each nucleus and then divided this value by its size in the same cell. The measurement of the FUrd intensity and the nucleolus sizes have been described in Chapter 2-Materials and Methods.

Figure 3.5 A and Table 3.5 illustrate the comparison between WT cells and sh2.43 shKATNAL-2 clone cells, where an increase appears from the clone. Furthermore, looking at the enriched growth media in WT and shKATNAL2 cells the mean values are 67.68 and 90.77 respectively and this is a significant increase that observing in the clone (p-value <0.0001). Additionally, the 10% and 20% serum concentrations in WT cells are rated with a p-value of 0.0016. In contrast, the cells in the restrictive growth media in WT dramatically decreased (mean value 20.03) compared to the normal (mean value 56.26) and enriched growth media. In shKATNAL2 cells the mean value in normal media is observed slightly higher (96.68) than the enriched growth media (90.77) (p-value is rated > 0.9999). Also, extremely significant is the p-value (<0.0001) between the same three growth media (0.5%, 10% and 20% serum concentrations) of both cell lines.

Moreover, Figure 3.5 B and Table 3.6 show the difference between the WT cells and the 8-8 shKATNAL-2 clone cells. The normal and enriched growth media in 8-8 shKATNAL-2 cells tend to have similar trend as in the 2.43 shKATNAL-2 cells, however the means in 8-8 clone cells impressively decreased with 56.33 and 55.84 respectively. Between the restrictive growth medias in WT cells and 8-8 shKATNAL-2 cells, the means of both growth media have negligible differences (21.18 and 23.76 accordingly). In opposition to graph A, the significance of both 0.5% serum concentrations between the WT cells and 8-8 shKATNAL-2 clone cells is rated with a p-value > 0.9999.
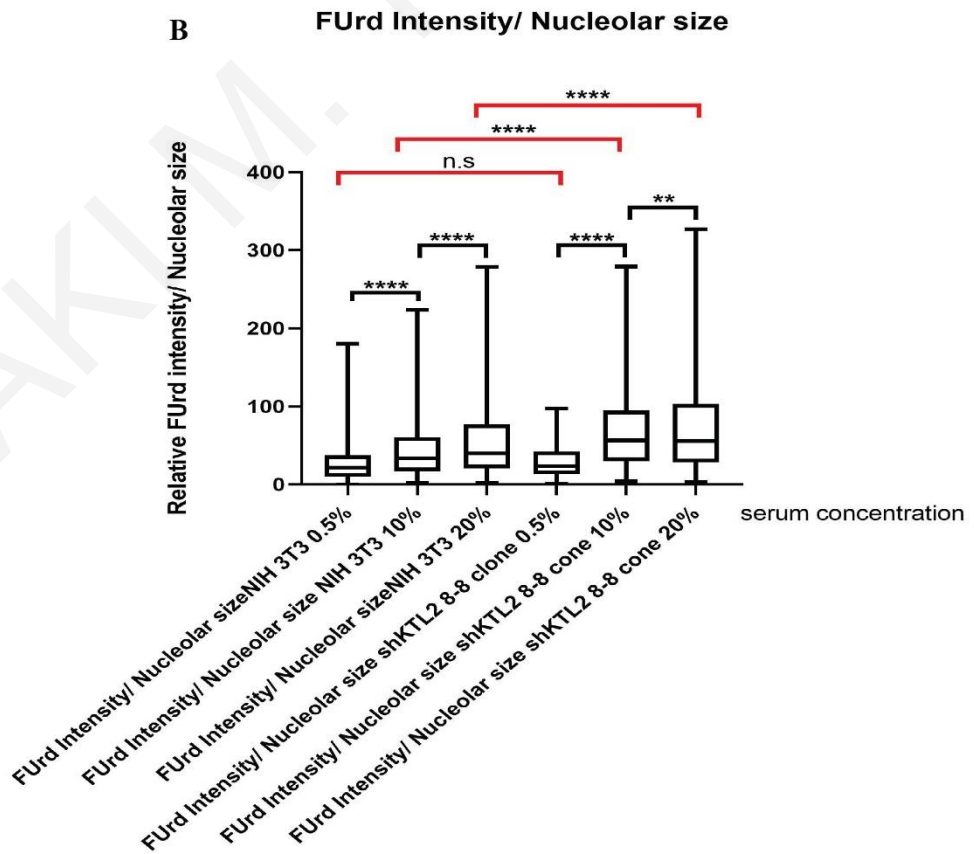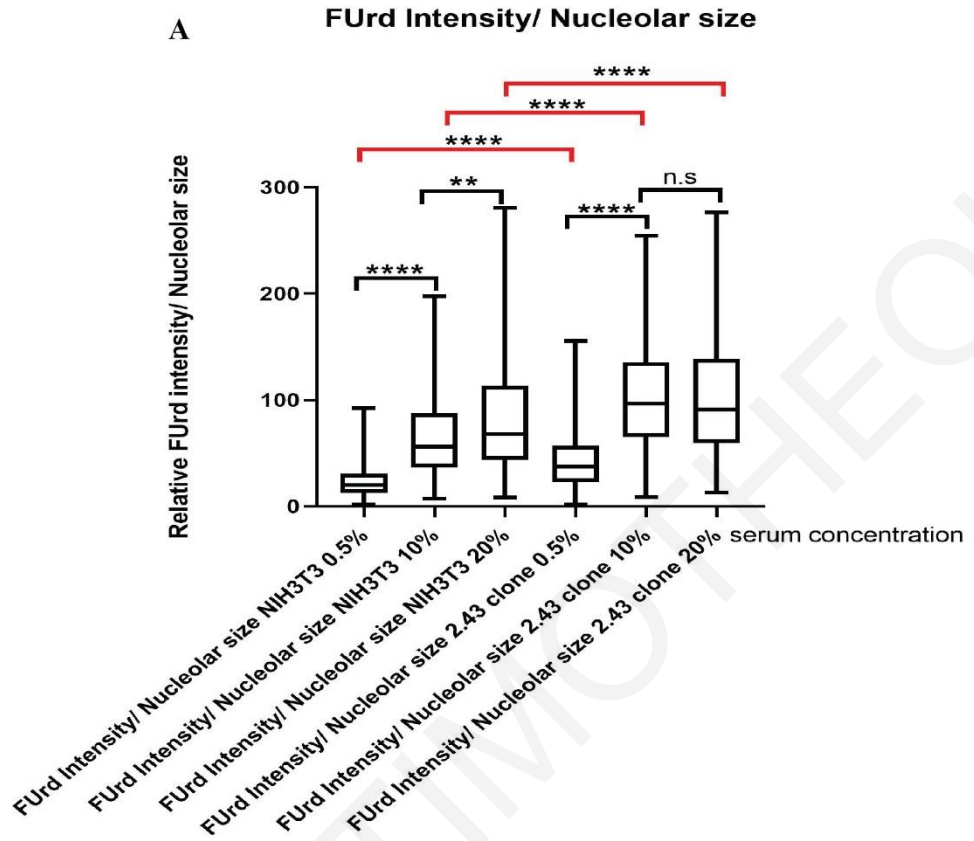
Figure 3.5

A FUrd Intensity/ Nucleolar size

B FUrd Intensity/ Nucleolar size

Figure 5 Quantitative and statistical analysis of FUrd intensity/ nucleolar size

A) *Graph A illustrates the differences between the WT cells and the shKATNAL-2 of the FUrd intensity/ nucleolar size. The 20% serum concentration of WT cells has a small number of cells, with the highest values near 300. Most values fluctuated near 100 for normal and enriched growth media, while in restrictive growth media most cells fluctuated under 50. However, in the 10% and 20% serum concentrations for silenced KATNAL-2 cells, most values vary from 1 to 100 and some other cells vary between 200 and 300. It is observed that the values of the three conditions in the shKATNAL-2 cells are increased, especially in 0.5% and 10% sera compared to WT cells. All the sera are statistically significant except the 10%-20% sera, which are not statistically significant.*

B) *The same pattern as graph A is maintained in graph B but most cells have values under 100, and others reach up to 300, like in the 20% serum concentration of the shKATNAL-2. In between the restrictive growth media in both cells is observed that most cells are near to 50 but in WT the maximum values are double than in shKATNAL-2 cells. However, the 0.5% serum in clone cells shows decreased values compared to the other sera in both cell lines. All serum concentrations differences are statistically significant except the 0,5% concentrations in both cell lines, which is opposite in Graph A.*

All statistical evaluations were performed One-way ANOVA assessed the statistical significance of differences with Tukey's correction. A p-value < 0.05 is regarded as statistically significant (*), <0.01 very significant (**), <0.001 highly significant (***), and <0.0001 extremely significant (****).

Table 3.5: Comparison of the distribution of the ratio of FUrd intensity per nucleolar size between WT cells and 2.43 shKATNAL-2 cells					
NIH 3T3 (WT control)			**2.43 shKATNAL-2**		
	0.5% serum conc.	**10% serum conc.**	**20% serum conc.**	**0.5% serum conc.**	**10% serum conc**	**20% serum conc.**
Mean	20.03	56.26	67.68	23.76	96.68	90.77
± SD	14.93	41.33	52.77	28.42	48.49	55.74

48

Table 3.6: Comparison of the distribution of the ratio of FUrd intensity per nucleolar size between WT cells and 8-8 shKATNAL-2 cells					
	NIH 3T3 (WT control)			8-8 shKATNAL-2		
	0.5% serum conc.	10% serum conc.	20% serum conc.	0.5% serum conc.	10% serum conc	20% serum conc.
Mean	21.18	33.33	39.36	23.76	56.33	55.84
± SD	20.98	39.53	52.62	20.57	51.40	67.24

3.4 Quantification of the number of nucleoli in each nucleus

Recent studies have elucidated that the nucleolar number is not static, and it is appeared to have a reduction in the number of nucleoli upon depletion of proteins required for ribosome biogenesis (Ogawa *et al.,* 2020). Generally, the larger size and higher number of nucleoli are detected in most tumor cells than the corresponding normal cells (Lo *et al.,* 2006).

The next part of the analysis focused on the number of nucleoli generated per nucleus. After the observation that the size of the nucleolus changed, subsequently implemented the counting of the total number of nucleoli per nuclei. Figure 3.6 illustrates the number of nucleoli in each cell line grown in different growth media (0.5%, 10% and 20% serum concentrations). Nucleoli shown in red indicates the FUrd incorporation to enable measurement. DNA was stained with Hoechst and displayed in blue and then the third horizontal series shows the overlay by the two colours.

Investigation of the images on IMARIS from all cell lines separately reveals a striking way that the 8-8 silencing-KATNAL-2 clone cells in all growth media possessed a visibly higher number of nucleoli in most cells, and it is evident from the 0.5% serum concentration (Fig. 3.6). As the concentration increases in the growth media, there is more nucleoli in 8-8 shKATNAL-2 clone cells, and the differences are distinct in the images.

The 2.43 shKATNAL-2 clone cells produce more nucleoli than WT cells, but the 8-8 shKATNAL-2 clone cells produce much more nucleoli than the WT and 2.43 shKATNAL-2 clone cells. However, the differences between the number of nucleoli in the 2.43 shKATNAL-
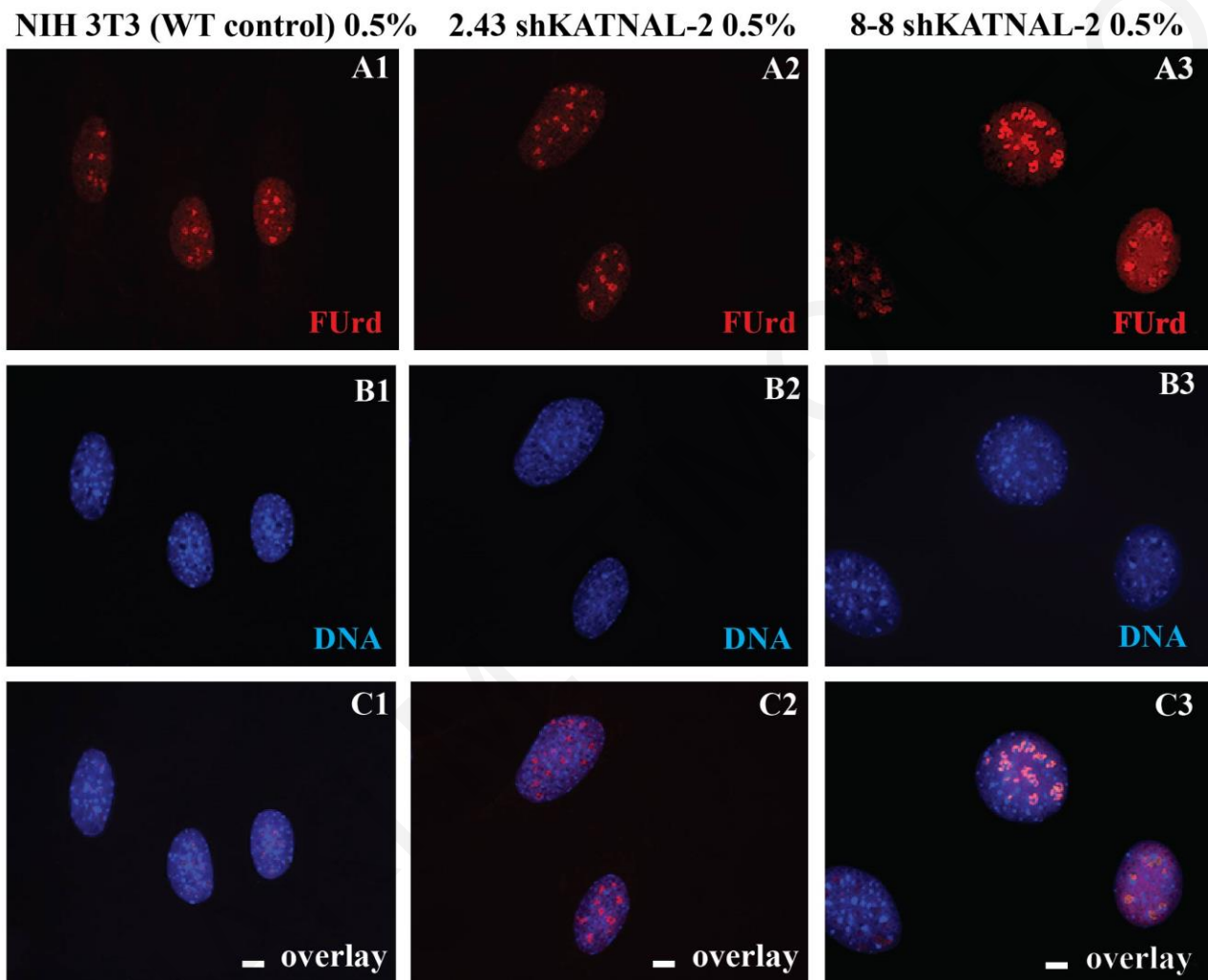
2 clone cells are more distinguishable as the concentration increases, but this is not observed in WT. Additionally, between both 10% and 20% serum concentration in WT cells, there is no obvious difference observed in the number of nucleoli.

The quantification of results in Fig. 3.7 A and Table 3.7 show the differences in the production of nucleoli per cell between the WT cells and the 2.43 shKATNAL-2 clone cells. If we focus on the restrictive, normal, and enriched growth media in WT cells, in that case, there is not a significant difference in the number of nucleoli as the serum concentration is increased. The mean values to is 8 for normal media and 7 for restrictive and enriched media (p-value 0.0934 for 10% and 20% serums, p-value 0.004 for 0.5% and 10% serums). On the other hand, the shKATNAL-2 cells have a constant increase between the three experiments compared to WT even though they have the same mean values in both cell lines. The differences in the numbers between the two cell lines are not significant. For example, the maximum value is 18 in enriched growth media in shKATNAL2 while in WT is 15 while, in normal medias are 15 for WT and 16 for shKATNAL2 cells. Nevertheless, there is no statistical significance between the same three growth media (p-value of 0.8952 for 0.5% serums, p-value 0.6530 for10% serums, and p-value >0.9999 for 20% serums).

If we take a look at Fig. 3.7 B, the significant differences in the nucleoli numbers between WT cells and 8-8 shKATNAL-2 cell line are perceived (Figure 3.7 B, Table 3.8). The mean value in WT is 7 for all growth mediums. However, the maximum values are negligible between the three experiments in WT (maximum value for 0.5% serum is 11, for 10% serum is 12 and for 20% serum is 17). Also, evaluations are not statistically significant with p-value 0.2285 between 0.5% and 10% sera and p-value 0.9989 between 10% and 20% serum. By contrast, in 8-8 shKATNAL-2 cells, there is an exponential increase in nucleoli in the three experiments compared to WT and 2.43 shKATNAL2 cells. Impressively, in the restrictive growth media (0.5% serum) in shKATNAL-2 cells outnumbered the mean value of the enriched growth media (20% serum) in WT, which did not happen in other parameters (mean for 0.5% serum in shKATNAL2 is 11 while in 20% serum in WT is 7). In normal and enriched growth media, the mean value is 13 and the maximum values are 19 and 22 respectively, which are remarkable compared to WT and 2.43 shKATNAL2 cells. The statistical significance between the same growth media in both cell lines rated extremely significant (p-value <0.0001), as well as the 0.5%-10% sera of the 8-8 shKATNAL-2 cells. To conclude, again we hypothesis that KATNAL2 plays essential role in the rRNA expression because in addition to the increase in the size of the nucleoli, at the same time there is a significant increase in the number of them.
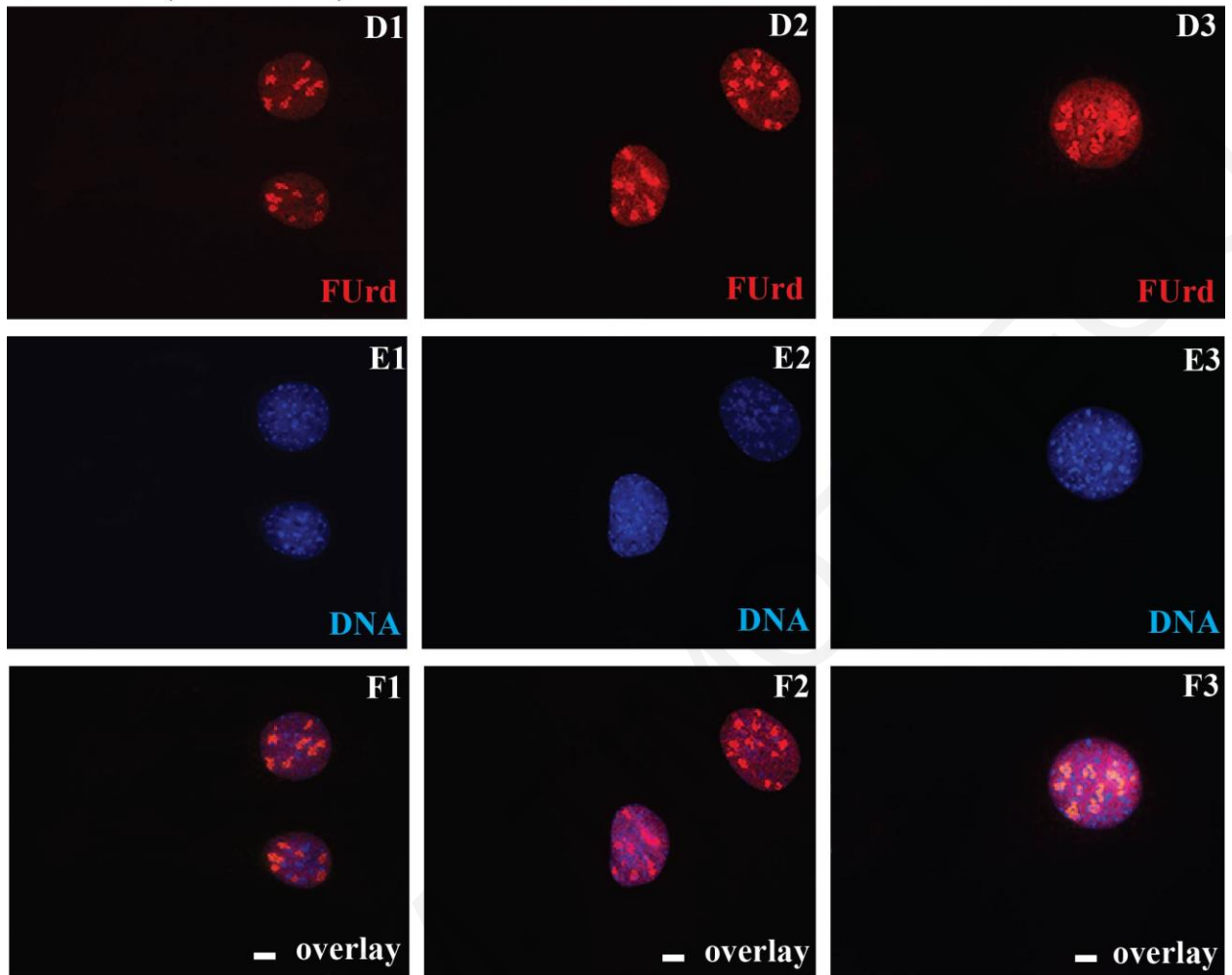
Figure 3.6

Nucleoli numbers

NIH 3T3 (WT control) 0.5%	2.43 shKATNAL-2 0.5%	8-8 shKATNAL-2 0.5%

NIH 3T3 (WT control) 10%   **2.43 shKATNAL-2 10%**   **8-8 shKATNAL-2 10%**

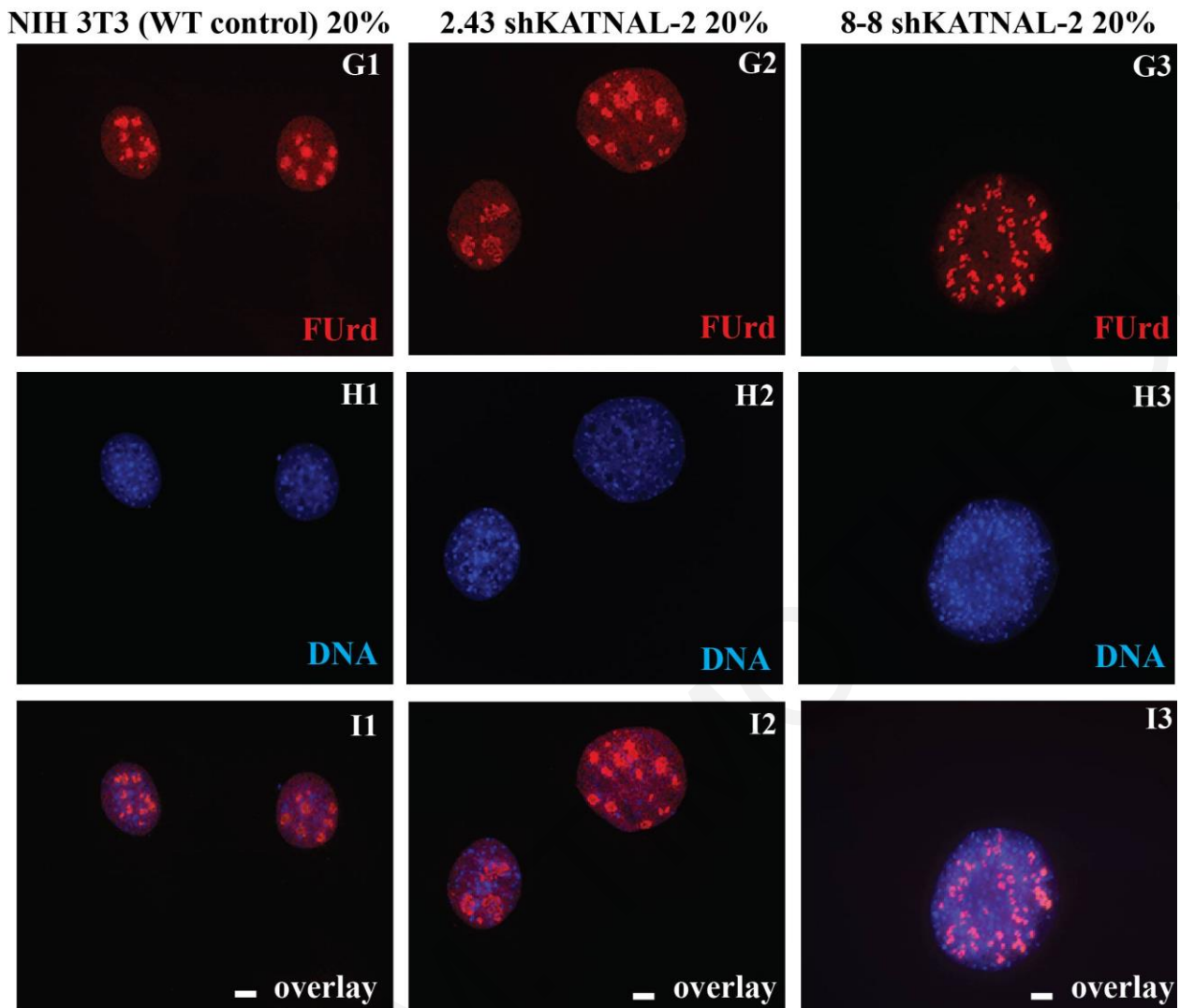| NIH 3T3 (WT control) 20% | 2.43 shKATNAL-2 20% | 8-8 shKATNAL-2 20% |

Figure 3.6 Visualisation of the number of nucleoli per cell produces in WT cells and silenced-KATNAL-2 clone.

(A1-I3) Evaluation of relative nucleoli numbers. Representative immunofluorescence images of cells cultured in three independent growth media: restrictive growth media (0.5% serum concentration), normal growth media (10%) and enriched growth media (20%). The first horizontal red images indicate the incorporation of FUrd into the nascent RNA, while the images with blue correspond to the DNA stained by Hoechst. Overlay of the two colours is also shown. Scale is 10μm.

(A, D, G) In general, there is an increase in the number of nucleoli in shKATNAL-2 cells compared to WT, however the 8-8 shKATNAL-2 clone cells outnumbered the other two cell lines. The differences in number of nucleoli are more distinct in the enriched growth media (20% serum) in the 8-8 shKATNAL-2 in between the 2.43 shKATNAL-2 clone cells and the WT. Among the WT and 8-8 shKATNAL-2 clone cells there is a notable increase in nucleoli number. The same happens with the 2.43 shKATNAL-2 cells and WT cells but the differences in the numbers are not particularly large.
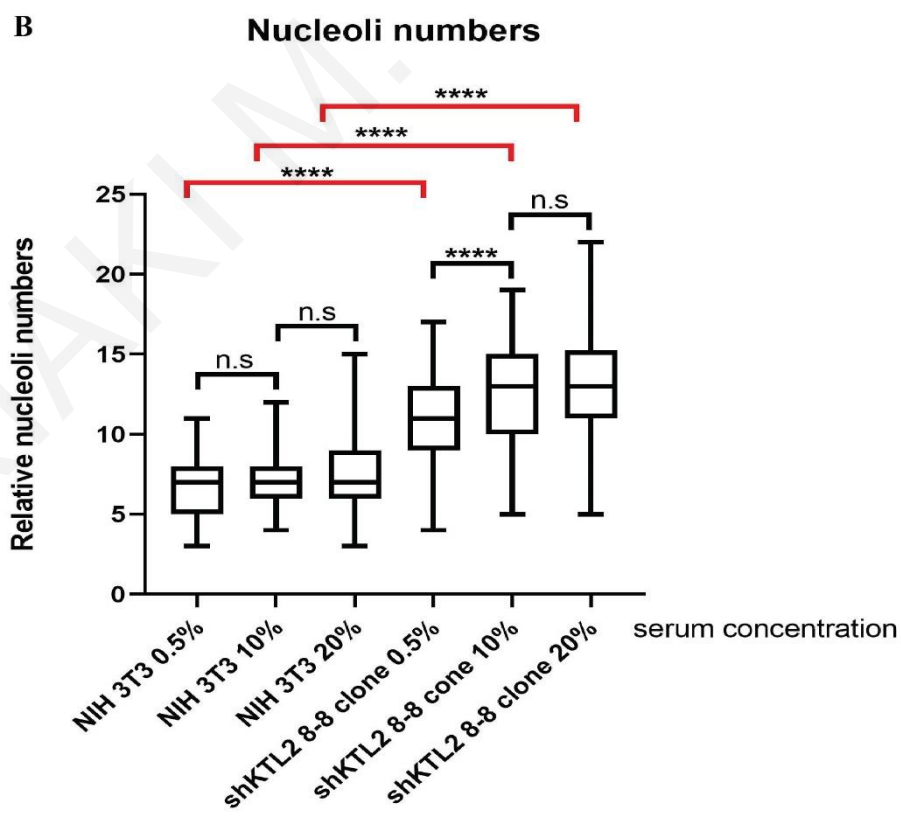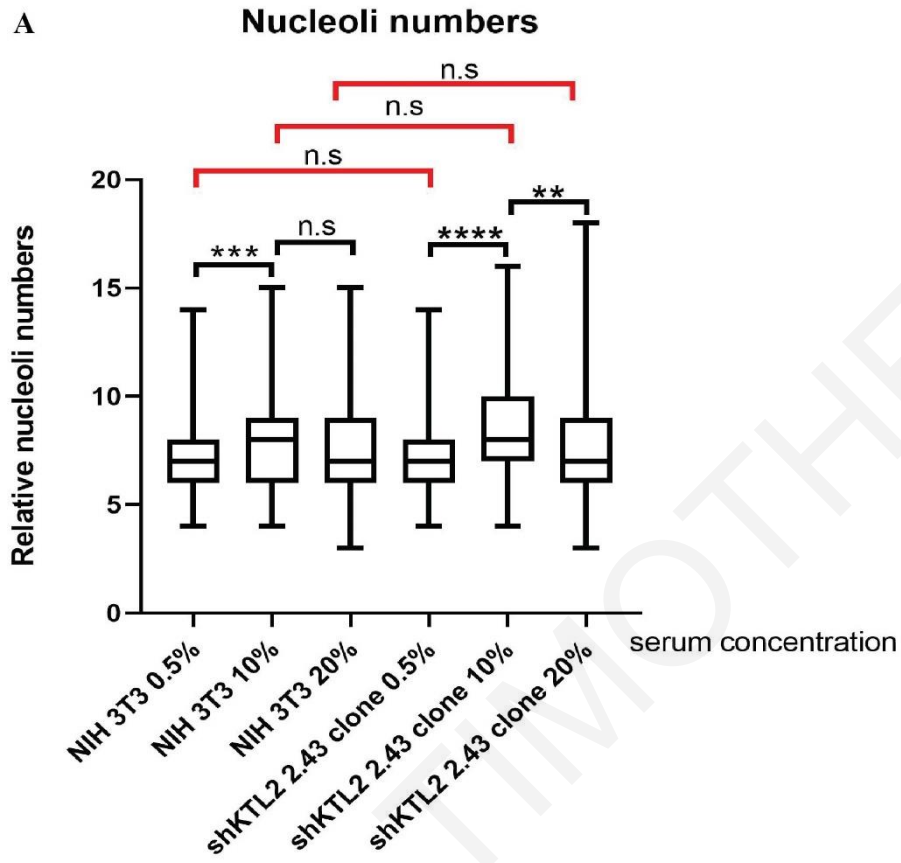
53

Figure_3.7

Table 3.7: Quantification of the number of nucleoli between WT and 2.43 shKATNAL-2 cells						
	NIH 3T3 (WT control)			8-8 shKATNAL-2		
	0.5% serum conc.	10% serum conc.	20% serum conc.	0.5% serum conc.	10% serum conc	20% serum conc.
Mean	7	8	7	7	8	7
± SD	1.786	2.098	2.212	1.920	2.233	2.521

Table 3.8: Quantification the number of nucleoli between WT and 8-8 shKATNAL-2 cells						
	NIH 3T3 (WT control)			8-8 shKATNAL-2		
	0.5% serum conc.	10% serum conc.	20% serum conc.	0.5% serum conc.	10% serum conc	20% serum conc.
Mean	7	7	7	11	13	13
± SD	1.938	1.703	2.116	2.9661	3.295	3.643

Figure 3.7 Quantification and statistical evaluation of the nucleoli numbers per cell.

A) *Graph A illustrates the quantification of the nuclei numbers per cell and per growth media in WT cells and 2.43 shKATNAL-2 clone cells. In WT cells we did not observe great increase between the restrictive growth media and the normal media nor between the normal and enriched growth media. The numbers of nucleoli that cells produce fluctuates from 5 to 15 for restrictive and normal growth media and over than 15 for enriched growth media. In contrast, the 2.43 shKATNAL-2 clone cells observed an upward trend in the number of nucleoli between the growth media related to WT which the nucleoli numbers are similar independently the growth media.*

B) *Graph B shows the difference in the numbers of nucleoli that each cell produces per growth media between WT cells and 8-8 shKATNAL-2 cell clone. In Graph B there is an increase trend in all growth media of WT cells that is in contrast with the WT cells in graph A. Comparing the cell lines, the 8-8 shKATNAL-2 clone cells, in graph B had been increased their nuclei markedly and there is a large difference with 2.43 shKATNAL-2 cells .Overall, we can suppose that in the absence of KATNAL 2 both clone cells produce a significant number of nucleoli, compared to WT but, 8-8 shKATNAL 2 cells to produce higher number of nucleoli compared the WT and 2.43 shKATNAL-2 cells.*

All statistical evaluations were performed One-way ANOVA assessed the statistical significance of differences with Tukey's correction. A p-value ＜0.05 is regarded as statistically significant (*), <0.01 very significant (**), <0.001 highly significant (***), and <0.0001 extremely significant (****).

Figure 3.5 Quantification analysis of the nuclei sizes

Recent studies support that the cell differentiation, development, and illness are all correlated with alterations in nuclear size and shape. Notably, cancer cells frequently exhibit altered nuclear morphology. Although the physiological effects of altered nuclear size and shape are largely unknown, they may have an impact on chromatin structure and gene expression (Jevtić *et al.,* 2014).

The last analysis of our research aims at the evaluation and quantification of the nucleus size. A logical explanation behind this concept is that since the size and number of nuclei in cells change, mainly in the absence of the KATNAL-2, the same can happen with the size of the nucleus.

Figure 3.8 demonstrates the nuclear size in each cell line in different growth media (0.5%, 10% and 20% serum concentrations). Nucleus with nucleoli which is shown in red indicates the FUrd incorporation and, simultaneously, the expression of rRNA (Fig. 3.5 A, D and G). DNA was stained with Hoechst and displayed in blue (Fig. 3.8 B, E and H), and then the third horizontal series shows the overlain by the two colours (C, F, and I). There is a significant increase in the nuclei size, as measured from the Hoechst-labeled images, specifically in enriched growth media of shKATNAL-2 cells compared to WT. The nuclei in normal and restrictive growth media in 8-8 shKATNAL-2 cells are slightly increase than the respectively growth media in 2.43 shKATNAL-2 cells.
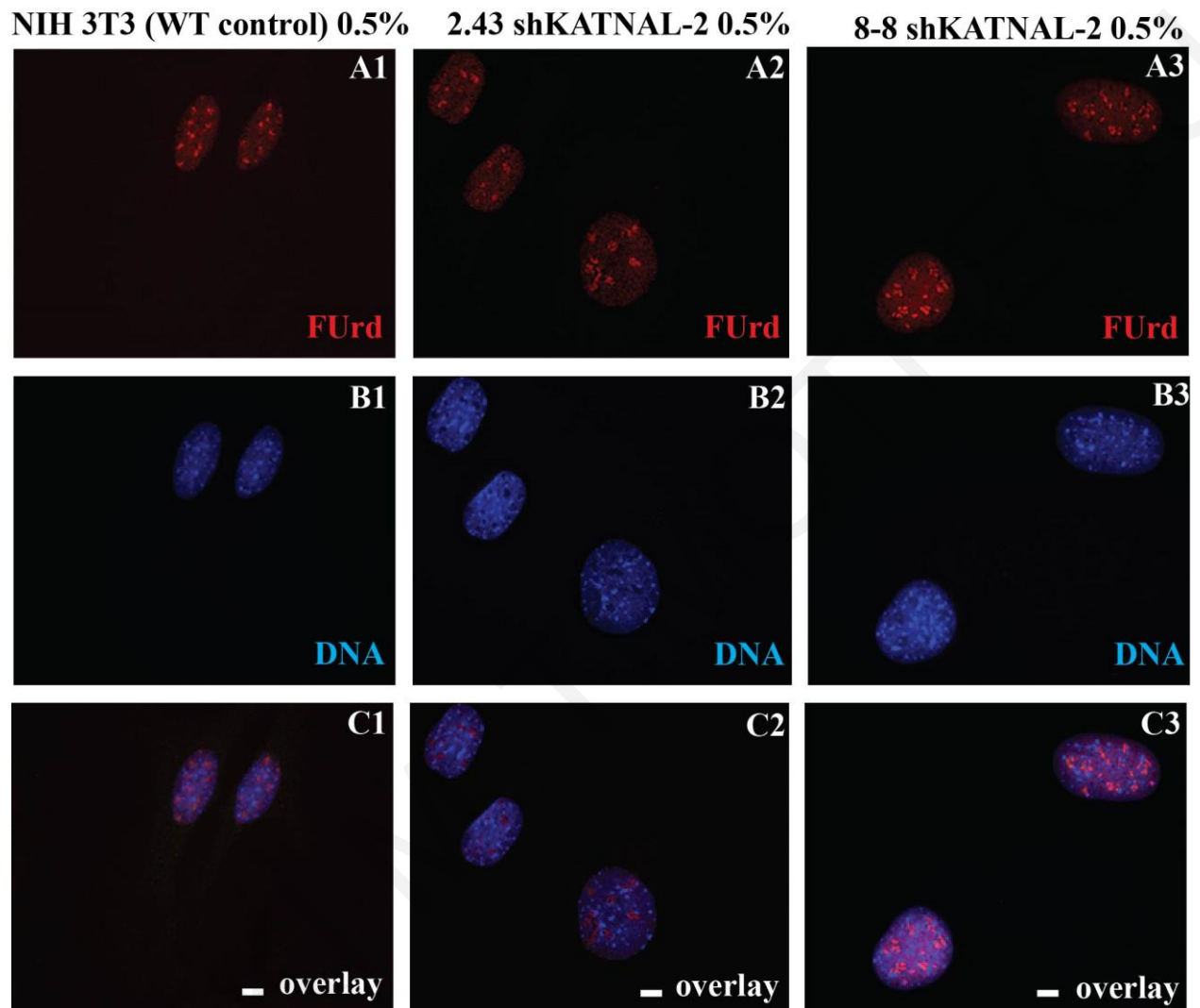
Figure 3.9 A and Table 3.9 A illustrate the nuclear size per growth media in WT cells and sh2.43 shKATNAL-2 clone cells. There is a 1.19-fold increase in the size of the nuclei in WT cells at the normal growth media compared to restrictive growth media (p-value 0.1450). At the same time, between normal and enriched growth media, there is a 1.3- fold increase (p-value 0.003) in WT cells. Although the restrictive and normal growth media in the shKATNAL-2 cells have slightly differences nevertheless, there is a 1.09-fold increase in normal media (p-value 0.7826), while between the normal and enriched growth media, there is a 1.21-fold increase from the enriched growth media (p-value <0.0001). Overall, comparing both cell lines, we can affirm that the shKATNAL-2 cells increased the size of nuclei more than the WT

cells. Between the restrictive and normal media in both cell lines we observe a 1.60-fold increase in shKATNAL2 cells compared to WT. (p-value 0.0213). A 1.67-fold increase is observed at 10% serum in shKATNAL2 compared to WT cells for the respectively 10% serum (p-value 0.2123). Moreover, between the enriched growth media of observed a respectable difference with 1.74-fold increase in shKATNAL2 cells compared to WT cells. (p-value 0.0028).

The results in Figure 3.9 B and Table 3.10 are more distinct between the two cell lines than in Graph A. There is an insignificant different between 0.5% and 10% growth mediums in WT (p-value 0.9819) as well as between normal and enriched growth mediums (p-value 0.1613). For example, there is a 1.04-fold increase from 10% to 0.5% sera, while it is observed a 1.17-fold increase from 20% to 10% sera. Looking at the shKATNAL-2 cells, there is a gradual increase in the sizes of nuclei as the concentration is increased compared to WT cells. Between 0.5% sera there is 1.6-fold increase from shKATNAL2 cells compared to WT cells (p-value <0.0001), while there is a 2-fold increase from 20% serum in shKATNAL2 than in 20% serum in WT cells (p-value <0.0001) At the same time, between the normal growth media there is a 1.67-fold increase in shKATNAL2 cells (p-value <0.0001). Overall, except for the size and number of nucleoli, we have now observed changes in the sizes of the nuclei in the absence of KATNAL2 mainly in enriched growth media.
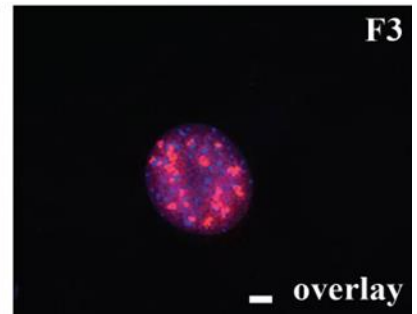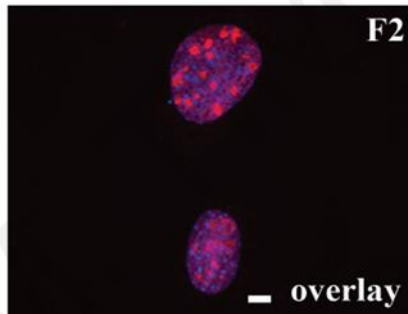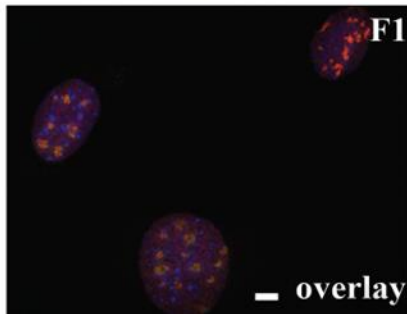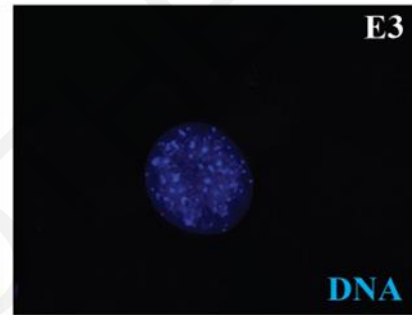
Figure 3.8

Nuclei sizes

NIH 3T3 (WT control) 10%	2.43 shKATNAL-2 10%	8-8 shKATNAL-2 10%
D1 — FUrd	D2 — FUrd	D3 — FUrd
E1 — DNA	E2 — DNA	E3 — DNA
F1 — overlay	F2 — overlay	F3 — overlay
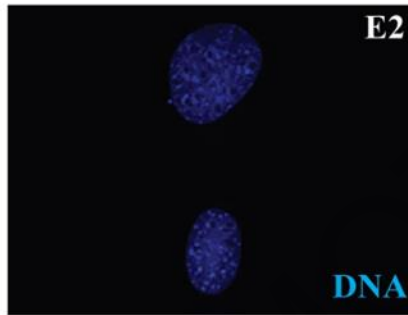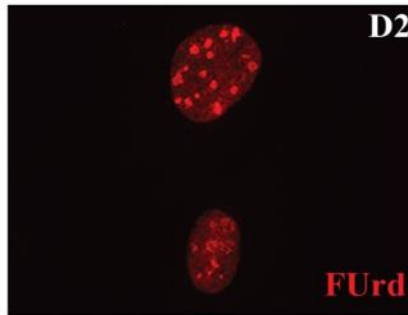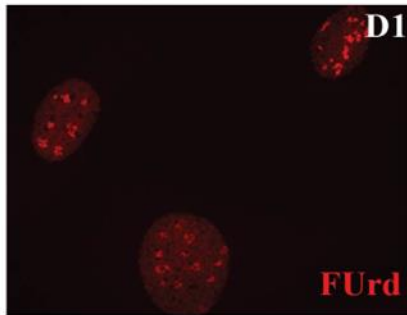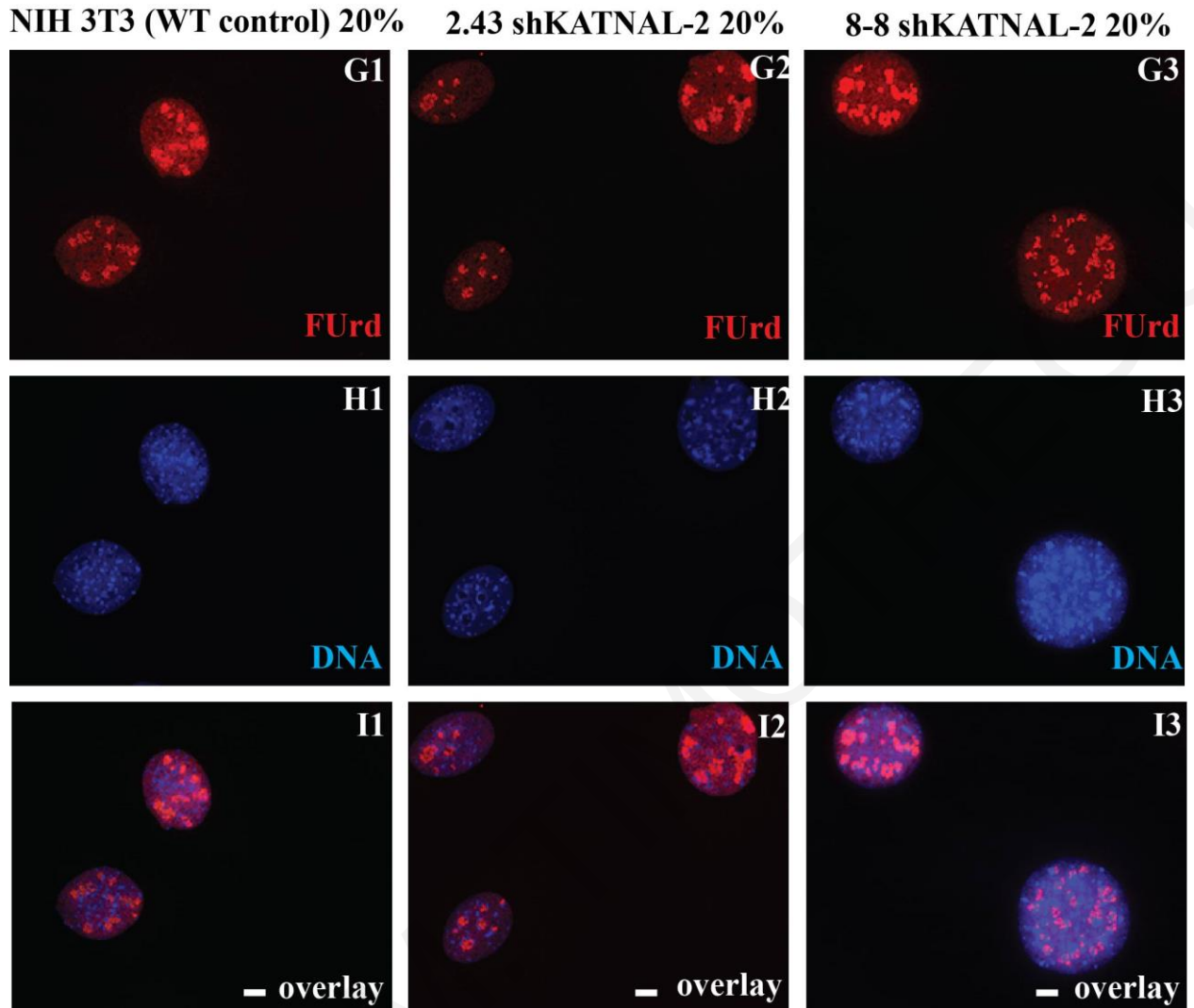
Figure 3.8 Visualization of the size of nuclei

(A1-I3) Observation of nuclear size. Representative immunofluorescence images of cells cultured in three independent growth media: restrictive growth media (0.5% serum concentration), normal growth media (10%) and enriched growth media (20%). Scale is 10μm.

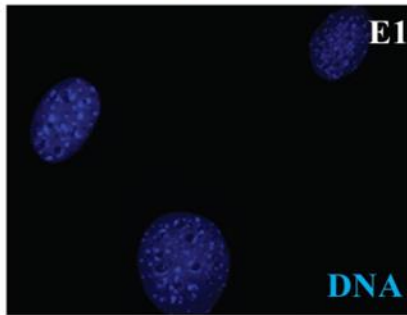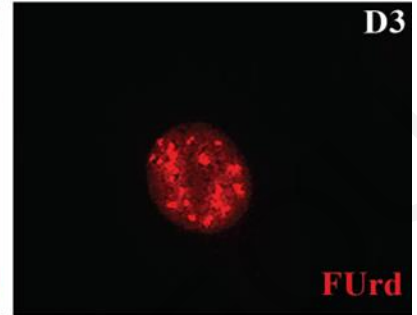*(A, D, G) Unconditionally, there is a significant increase in the size of nuclei in shKATNAL-2 cells compared to WT, however the 8-8 shKATNAL-2 clone cells outnumbered the other two cell lines. Among the WT and 8-8 shKATNAL-2 clone cells there is an impressive increase in the size of nucleus. The same happens with the 2.43 shKATNAL-2 cells and WT cells but the differences in the numbers are not particularly big.*

Figure 3.9

A

Nuclear size

B

Nuclear size

Figure 3.9 Quantification and statistical evaluation of the size of nuclei

A) *Graph A displays the nuclear size differences between the WT and 2.43 shKATNAL-2 clone cells in three independent experiments. The enriched growth media (20% serum) in both cell lines remain increased, with the maximum number of nuclei in WT cells being near 15, while shKATNAL-2 cells are slightly more than 15. In contrast, the restrictive and normal growth media in shKATNAL-2 cells outnumber the growth media in WT but with a slightly different.*
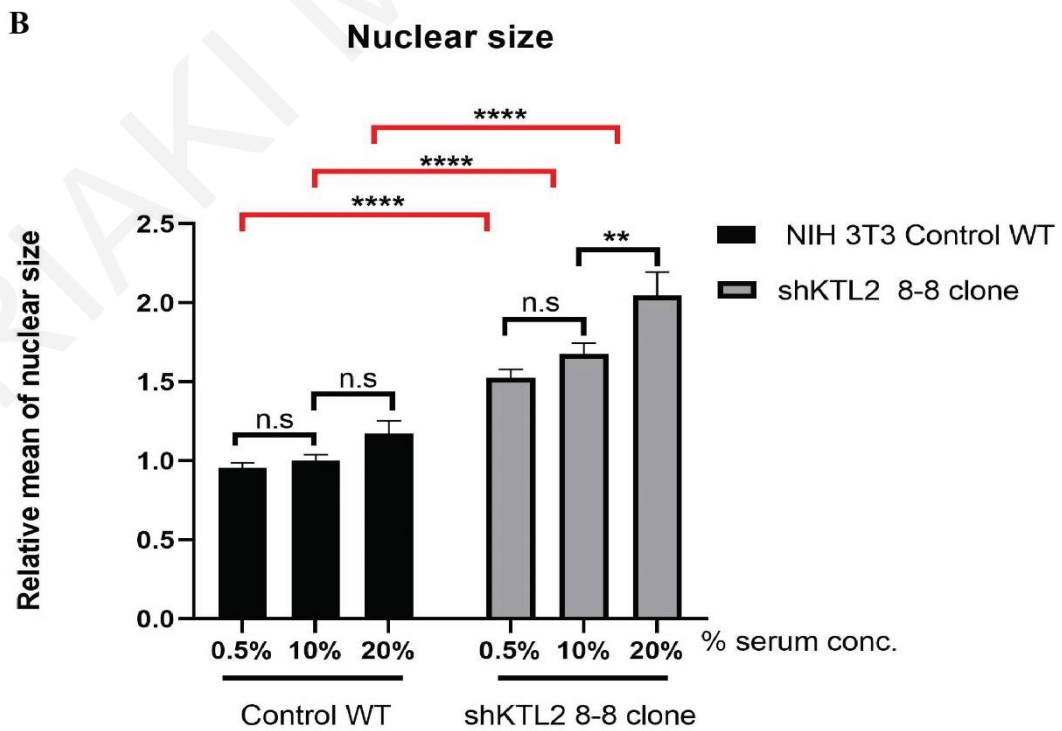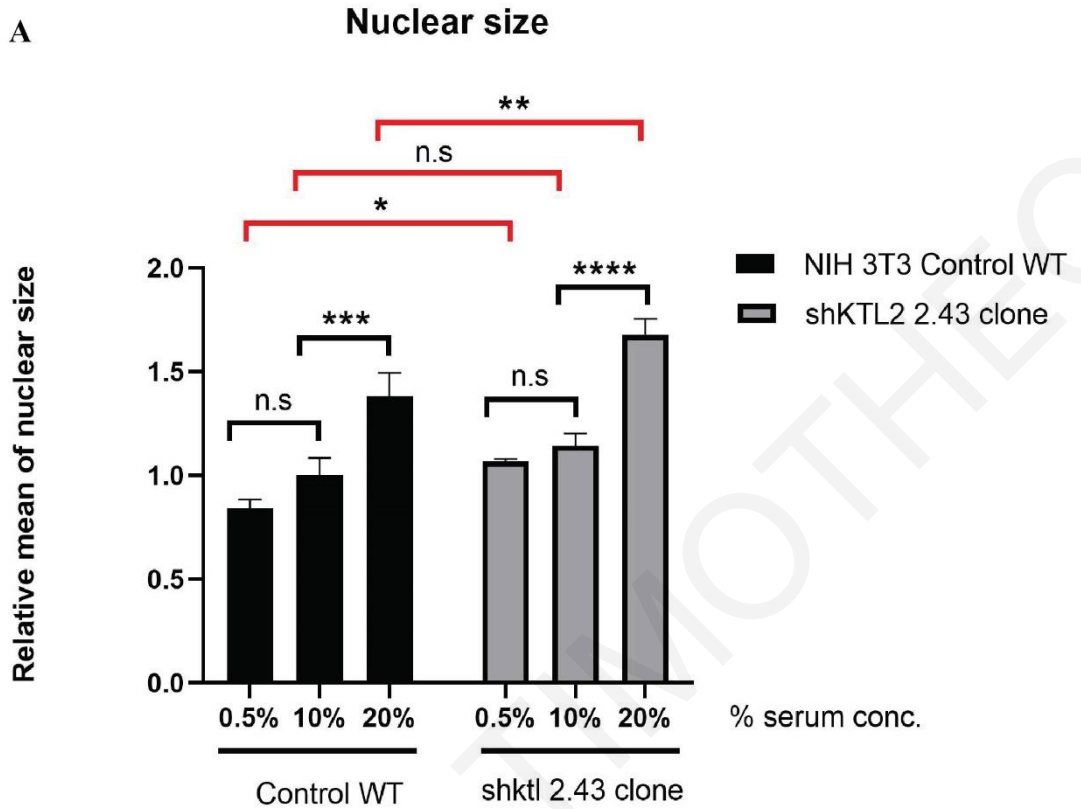
B) *In graph B, the shKATNAL-2 nuclei far exceed in size compared to WT in all growth media. The 20% serum in clone cells is double in size of the 20% serum in WT, and the restrictive and normal growth media significantly increase compared to WT. In conclusion, it is observed repeatedly that the absence of KATNAL 2 affects the nuclei size at all growth media.*

Two-way ANOVA assessed the statistical significance of differences with Tukey's correction. A p-value <0.05 is regarded as statistically significant (*), <0.01 very significant (**), <0.001 highly significant (***), and <0.0001 extremely significant (****).

Table 3.9: Evaluation and quantification of the size of nuclei between WT and 2.43 shKATNAL-2 cells

	NIH 3T3 (WT control)			8-8 shKATNAL-2		
	0.5% serum conc.	10% serum conc.	20% serum conc.	0.5% serum conc.	10% serum conc	20% serum conc.
Mean	0.842706128	1	1.383462697	1.067446236	1.142735297	1.678946552
± SD	0.039795946	0.084234769	0.111196043	0.012150072	0.059163999	0.075744793

Table 3.10: Evaluation and quantification of the size of nuclei between WT and 8-8 shKATNAL-2 cells

	NIH 3T3 (WT control)			8-8 shKATNAL-2		
	0.5% serum conc.	10% serum conc.	20% serum conc.	0.5% serum conc.	10% serum conc	20% serum conc.
Mean	0.95609038	1	1.17222614	1.52593745	1.67505846	2.04771324
± SD	0.03140688	0.03850751	0.08035336	0.05336107	0.07086964	0.14698252

DISCUSSION

Katanins have been functionally implicated in critical cellular and developmental processes involving microtubule (MT) remodelling, including spindle assembly in mitosis and meiosis, flagella and cilia assembly and disassembly, and neural morphogenesis. Unexpectedly, a portion of KATNAL2 resides in the nucleolus, and this new discovering is trigger for additional research about its role in the nucleolus, more specifically in rRNA transcription.

The primary purpose of this study is to monitor the expression of the rRNA and simultaneously to study the role of KATNAL2 in ribosomal gene transcription. To achieve that, hosts of Santama's Laboratory performed three independent experiments using wild-type and silenced-KATNAl2 clone-cells cultured in three different serum concentrations of 0.5% (restrictive growth media), 10% (normal growth media) and 20% (enriched growth media), (n=100 per condition and per cell line).

As a complement to other approaches, such as Northern blot and quantitative RT-PCR which are standard methods used to measure gene expression levels, the cells were incubated shortly with 5-fluorouridine, incorporated into a nascent RNA as an analogue to uracil, to assess total rRNA production. In this thesis, the quantitative evaluation was completed by the investigation of statistical analysis of FUrd intensity, the nucleolar and nuclear size, the number of nucleoli and FUrd intensity/size of the nucleolus. The IMARIS software was used to analyze microscope-captured pictures, and GraphPad Prism 8 was used for graph presentation and statistical analysis of quantifications.

According to the results, the purpose of this study was successful in evaluating and quantifying the parameters that were mentioned above for the measurement of the rRNA expression. Since the rRNA is the most abundant type of RNA in the intracellular matrix and comprised about 80% of the total RNA (Singh *et al.,* 2018), in this study we monitored the expression pre-RNA (47S) as well as the different types of RNA that may have been expressed in the three independent experiments in WT and shKATNAL-2 cell lines.

The first approach is about the quantification of FUrd intensity. The results revealed that there is a stunning increase of FUrd intensity mainly in shKATNAL2 clone cells compared to WT cells. Observing these results, we understand that FUrd is incorporated into the nascent RNA successfully and this intensity in the shKATNAL-2 cells indicates the rRNA expression.

It is significant to mention that, using FUrd into our cell lines, does not know precisely which species of RNA are produced, it will be a mix of the pre-RNA (47S), downstream intermediates and mature rRNAs. It has been shown that, 5-FU misincorporation can result in toxicity to RNA at several levels. It not only inhibits the processing of pre-rRNA into mature rRNA, but also disrupts post-transcriptional modification of tRNAs and the assembly and activity of snRNA/protein complexes, thereby inhibiting splicing of pre-mRNA (Therizols *et al.,* 2022). In this study, is confirmed that there is incorporation of FUrd into the newly synthesized rRNA because we observed high intensity since increase in rRNA transcription.

Interesting is the fact that we observed change in the size of nucleoli specifically in KATNAL2-silenced cells. Nucleoli has been enlarged in shKATNAL-2 cells compared to WT. The increase in the size of nucleoli is more obvious in the enriched growth media in all cell lines. Cells that are cultured in enriched growth media, might use excess growth factors and this led to increase rRNA expression. In shKATNAL-2 cells there is a significant increase in size of nucleolus in enriched growth medias compared to the respectively growth media in WT. Based on studies, the physical separation of the 3 nucleolar sub-compartments is possible due to the presence of immiscible liquid phases. These liquid-like phases (LLPS) are formed by specific heterotypic and homotypic electrostatic interactions between components of the nucleolar sub-compartments and thus allowing for their segregation the liquid-phase separation that leads to the assembly of nucleolar regions is facilitated by the presence of pre-rRNA (Navarro and Sorrell., 2023). LLPS plays a significant role in transcription, genome organization, immune response and cell signaling, and its dysregulation may cause neurodegenerative diseases and cancers (Luo *et al.,* 2021). Mammalian cells with increased rDNA transcription usually contain large and irregular nucleoli likely due to multiple liquid-phase separation nucleation events. These morphological alterations in the distribution of nucleolar sub-compartments are characteristic and indicative of nucleolar stress. Nucleolar stress can be visualized using immunofluorescence of nucleolar resident proteins such as NPM1(GC marker) and fibrillarin (DFC marker) (Navarro and Sorrell, 2023). Complementary research that confirms the enlargement of nucleoli is performed by members of the Santama laboratory by employing confocal analysis of nucleoli in KATNAL2-silenced cells. The results indicated that the silencing of KATNAL2 resulted in profound morphological changes in the structure of the nucleoli. Nucleoli were enlarged in comparison with wild-type, DFC marker protein fibrillarin had a more peripheral localization and heterochromatin masses surrounding the nucleoli were markedly reduced. Further analysis by Electron Microscopy confirmed

changes in the fine structure of nucleoli and indicated that the DFC was expanded at the expense of the FC. Taking these results together, we hypothesised that the increase in the size of nucleolus is cause by stress especially the cells cultured in enriched growth media where they have more factors. Additionally, the nucleoli of shKATNAL2 cells present increase in their size, therefore, the absence of KATNAL-2 affecting in some way the transcription and cause stress to the nucleoli.

In this work, we observed that there is a difference in the size of the nucleoli between silenced-shKATNAL2 clones, but not as much as compared to WT cells. Also, the size of nucleolus contributes to the rRNA transcription since the intensity is higher in larger nucleoli as the results indicates. The measurements of intensity per surface of each nucleolus are shown to increase and this is justifying by the impressively increased mean values of shKATNAL2 cells compared to WT cells. A future approach to confirm these results would be RNA metabolic labelling. Metabolic labeling refers to approaches that utilize the endogenous synthesis and modification machinery of live cells to add detection or affinity tags into biomolecules. Typically, this is performed by cultivating cells or organisms in conditions containing a tagged chemical analog of a certain natural molecular building block (e.g., amino acid, nucleotide, carbohydrate). Cells use the chemical analog instead of the natural biomolecule to synthesize or modify proteins, nucleic acids, etc. Metabolic labeling is a powerful strategy because it is simple to perform and enables measurement of metabolic rates and detection of biologically relevant interactions in vivo.

Nucleolus is a highly responsive organelle that integrates signals from a vast network of cellular processes. In this work, we observed a significant increase in nucleoli numbers in shKATNAL-2 clone cells, particularly in 8-8 shKATNAL2 clone cells compared to WT and 2.43 shKATNAL-2 cells. Based on the bibliography (Ogawa *et al.,* 2021), if there is a depletion of r-proteins (ribosomal proteins) it is observed a decrease in the number of nucleoli. The silencing of KATNAL-2 indicated the opposite effect where the nucleoli increased. Therefore, KATNAL-2 may not be a r-protein but implicates in ribosomal biogenesis. KATNAL2 is highly enriched in the nucleolus, particularly in the chromatin fraction, like nucleolar proteins UBF, fibrillarin, treacle and RNA Pol I (unpublished results). Therefore, silencing KATNAL2 may affect the binding on chromatin, which may impact rRNA transcription. Generally, the stress that is generated by the absence of KATNA2 is a critical reason for significant changes in the cells.

65

The last parameter that we investigated was the size of the nuclei. We observe that the number and size of nucleoli are increase in the absence of KATNAL2, we were curious if the nuclei size will be increased too. Impressively, the nuclei size is also increased again in shKATNAL-2 cells compared to WT. In addition, a strong correlation between nuclear size, RNA transcription levels and cell size has been found. It is therefore possible that larger nuclei facilitate the increase in transcription that is required in larger cells. Additionally, the volume of the nucleus might be important for maintaining nuclear compartments, such as the nucleolus, and the activity of enzymes such as DNA polymerase, which are sensitive to macromolecular crowding. Although the mechanisms that control nuclear volume remain unclear, the existence of a karyoplasmic ratio suggests that nuclear size is important for cell function (Webster *et al.*, 2009).

ABBREVIATIONS

ABBREVIATION	MEANING
FUrd	5-fluorouridine
shKATNAL-2	Silenced-Katanin-like-2
UBF	Upstream binding factor
IMARIS	Interactive Microscopy Image Analysis software
WT	Wild type
FC	Fibrillar component
FC	Dense fibrillar component
GC	Granular component
CDK	Cyclin dependent Kinase
Pol (I, II, III)	Polymerase I, II, III
UCE	Upstream control element
PIC	Pre-initiation complex
TBP	TATA-binding protein
LLPS	Liquid-Like Phases
RFB	Replication fork barrier
TTF1	Transcription terminal factor

BIBLIOGRAPHY

Hariharan, N. and Sussman, M.A. (2014) 'Stressing on the nucleolus in cardiovascular disease', *Biochimica et Biophysica Acta (BBA) - Molecular Basis of Disease*, 1842(6), pp. 798–801. doi:10.1016/j.bbadis.2013.09.016.

Hernandez-Verdun, D., Roussel, P.,Thiry, M., Sirri, V. and Lafontaine, D.L.J. (2010) 'The nucleolus: Structure/function relationship in RNA metabolism', *Wiley Interdisciplinary Reviews: RNA*, 1(3), pp. 415–431. doi:10.1002/wrna.39.

Hori, Y., Engel, C. and Kobayashi, T. (2023) 'Regulation of ribosomal RNA gene copy number, transcription and nucleolus organization in Eukaryotes', *Nature Reviews Molecular Cell Biology*. doi:10.1038/s41580-022-00573-9.

Iarovaia, O.V., Minina, E.P., Sheval, E.V, Onichtchouk, D., Dokudovskaya, S., Razin, S.V. and Vassetzky, Y.S. (2019) 'Nucleolus: A central hub for nuclear functions', *Trends in Cell Biology*, 29(8), pp. 647–659. doi:10.1016/j.tcb.2019.04.003.

Jevtić, P., Edens, L.J., Vuković, L.D. and Levy, D.L. (2014). 'Sizing and shaping the nucleus: mechanisms and significance'. *Curr Opin Cell Biol*,28, pp.16-27

Lafontaine, D.L. (2020) 'The nucleolus as a multiphase liquid condensate', *Nature Reviews Molecular Cell Biology*, 22(3), pp. 165–182. doi:10.1038/s41580-020-0272-6

Lo, S.J., Lee, C.-C. and Lai, H.-J. (2006) 'The nucleolus: Reviewing oldies to have new understandings', *Cell Research*, 16(6), pp. 530–538. doi:10.1038/sj.cr.7310070

Leung, A.K and Lamond, A, I. (2003) 'The dynamics of the nucleolus'. *Crit Rev Eukaryot Gene Expr*,13(1), pp. 39-54. https://doi.org/10.1615/critreveukaryotgeneexpr.v13.i1.40

Navarro, C. (2019). 'The Nucleolus'. *Trends in Genetics*.35(10), pp.709. https://doi.org/10.1016/j.tig.2019.08.001

Núñez, V.L., Wong, M.S., Ferguson, L.L., Hein, N., George, A.J. and Hannan, K,M. (2018) 'New roles for the nucleolus in health and disease', *BioEssays*, 40(5), p. 1700233. doi:10.1002/bies.201700233.

Ogawa, L.M. *et al.* (2021) 'Increased numbers of nucleoli in a genome-wide rnai screen reveal proteins that link the cell cycle to RNA polymerase I transcription', *Molecular Biology of the Cell*, 32(9), pp. 956–973. doi:10.1091/mbc.e20-10-0670.

Pederson, T. (1998) 'The plurifunctional nucleolus', *Nucleic Acids Research*, 26(17), pp. 3871–3876. doi:10.1093/nar/26.17.3871.

Salvetti, A. and Greco, A. (2014) 'Viruses and the nucleolus: The fatal attraction', *Biochimica et Biophysica Acta (BBA) - Molecular Basis of Disease*, 1842(6), pp. 840–847. doi:10.1016/j.bbadis.2013.12.010.

Singh, K.P., Miaskowski, C., Dhruva, A.A., Flowers, E. and Kober, K.M. (2018) 'Mechanisms and measurement of changes in gene expression', *Biological Research for Nursing*, 20(4), pp. 369–382. doi:10.1177/1099800418772161.

Therizols, G., Bash-Imam, Z., Panthu, B. *et al.*, (2022). 'Alteration of ribosome function upon 5-fluorouracil treatment favors cancer cell drug-tolerance'. *Nat Commun* (13)173 https://doi.org/10.1038/s41467-021-27847-8

Tsoi, H. and Chan, H.Y. (2014) 'Roles of the nucleolus in the CAG RNA-mediated toxicity', *Biochimica et Biophysica Acta (BBA) - Molecular Basis of Disease*, 1842(6), pp. 779–784. doi:10.1016/j.bbadis.

Ververis, A., Christodoulou, A., Christoforou, M., Kamilari, C., Lederer, C. W. and Santama, N.
(2015) 'A novel family of Katanin-like 2 protein isoforms (KATNAL2), interacting with

nucleotide-binding proteins nubp1 and nubp2, are key regulators of different MT-based
   processes
in mammalian cells', *Cellular and Molecular Life Sciences*, 73(1), pp. 163–184.
doi:10.1007/s00018-015-1980-5

Webster, M., Witkin, K.L. and Cohen-Fix, O. (2009) 'Sizing up the nucleus: Nuclear shape,
   size
and nuclear-envelope assembly', *Journal of Cell Science*, 122(10), pp. 1477–1486.
doi:10.1242/jcs.037333

Willsey, H.R.*,* Walentek, P., Exner, R.T.C., Xu, Y., Lane, A.B., Harland, R.M., Heald, R. and
Santama, N.*,* (2018) 'Katanin-like protein Katnal2 is required for ciliogenesis and brain
development in xenopus embryos', *Developmental Biology*, 442(2), pp. 276–287.
doi:10.1016/j.ydbio.2018.08.002

Useful Websites:

 Microscopy Image Analysis Software - Imaris - Oxford Instruments (oxinst.com)

Metabolic Labeling and Chemoselective Ligation | Thermo Fisher Scientific - CY